Published in Vadose Zone Journal 10, issue 3, 867-883, 2011
which should be used for any reference to this work

Chemical and Biological Gradients along the Damma Glacier Soil Chronosequence, Switzerland

Stefano M. Bernasconi*, Andreas Bauder, Bernard Bourdon, Ivano Brunner, Else Bünemann, Iso Christl, Nicolas Derungs, Peter Edwards, Daniel Farinotti, Beat Frey, Emmanuel Frossard, Gerhard Furrer, Merle Gierga, Hans Göransson, Kathy Gülland, Frank Hagedorn, Irka Hajdas, Ruth Hindshaw, Susan Ivy-Ochs, Jan Jansa, Tobias Jonas, Mirjam Kiczka, Ruben Kretzschmar, Emmanuel Lemarchand, Jörg Luster, Jan Magnusson, Edward A.D. Mitchell, Harry Olde Venterink, Michael Plötze, Ben Reynolds, Rienk H. Smittenberg, Manfred Stähli, Federica Tamburini, Edward T. Tipper, Lukas Wacker, Monika Welc, Jan G. Wiederhold, Josef Zeyer, Stefan Zimmermann, Anita Zumsteg

Soils are the product of a complex suite of chemical, biological, and physical processes. In spite of the importance of soils for society and for sustaining life on earth, our knowledge of soil formation rates and of the influence of biological activity on mineral weathering and geochemical cycles is still limited. In this paper we provide a description of the Damma Glacier Critical Zone Observatory and present a first synthesis of our multidisciplinary studies of the 150-yr soil chronosequence. The aim of our research was to improve our understanding of ecosystem development on a barren substrate and the early evolution of soils and to evaluate the influence of biological activity on weathering rates. Soil pH, cation exchange capacity, biomass, bacterial and fungal populations, and soil organic matter show clear gradients related to soil age, in spite of the extreme heterogeneity of the ecosystem. The bulk mineralogy and inorganic geochemistry of the soils, in contrast, are independent of soil age and only in older soils (>100 yr) is incipient weathering observed, mainly as a decreasing content in albite and biotite by coincidental formation of secondary chlorites in the clay fraction. Further, we document the rapid evolution of microbial and plant communities along the chronosequence.

This study describes the main features of the Damma glacier Critical Zone Observatory and its 150-year long soil chronosequence. We focus on early soil- and ecosystem genesis and document the rapid biological evolution and its influence on the chemistry of the soils and on chemical weathering.

Abbreviations: BS, base saturation; CEC_{eff}, effective cation exchange capacity; CIA, chemical index of al teration; ICP–OES, inductively coupled plasma optical emission spectrometry; LIA, Little Ice Age; PCA, principal component analysis; PCR, polymerase chain reaction; PLFA, phospholipid fatty acids; XRF, X-ray fluorescence spectroscopy; RDA, redundancy analysis; rfus, relative migration units; SOM, soil organic matter; TN, total N; TOC, total organic C; T-RF, terminal restriction fragment; T-RFLP, terminal restriction fragment length polymorphism.

Studies of ecosystems that integrate hydrological, biological, and earth system sciences are a challenging but also a promising avenue to improve our knowledge of ecosystem functioning, regulation, and evolution. The combination of different tools and scientific approaches can provide new insights into the cycling of elements and their influence on ecosystem development at the Earth's surface beyond what could be learned through disciplinary studies alone. An increasing number of multidisciplinary studies are being performed, as documented in this issue, to understand processes occurring in the Earth's critical zone, which is defined as the terrestrial environment from the top of the vegetation to the base of the groundwater zone (National Research Council Committee on Basic Research Opportunities in the Earth Sciences, 2001). This contribution describes the first results of a multidisciplinary study on a deglaciation chronosequence focusing on the understanding of the initial phases of ecosystem development, weathering, and soil formation.

S.M. Bernasconi, M. Gierga, R.H. Smittenberg, Geological Inst., ETH Zürich, Sonneggstrasse 5, 8092 Zürich, Switzerland; A. Bauder and D. Farinotti, Lab. of Hydraulics, Hydrology and Glaciology (VAW), ETH Zürich, Gloriastrasse 37/39, 8092 Zürich Switzerland; B. Bourdon, R. Hindshaw, M. Kiczka, E. Lemarchand, B. Reynolds, E.T. Tipper, J.G. Wiederhold, Inst. of Geochemistry and Petrology, ETH Zürich, Clausiusstrasse 25, 8092 Zürich Switzerland; I. Brunner, B. Frey, K. Gülland, F. Hagedorn, J. Luster, S. Zimmermann, A. Zumsteg, Soil Sci., WSL Swiss Federal Inst. for Forest, Snow and Landscape Res., Zürcherstrasse 111, 8903 Birmensdorf, Switzerland; E. Bünemann, E. Frossard, J. Jansa, F. Tamburini, M. Welc, Inst. of Agric. Sci., ETH Zürich, Eschikon 33, 8315 Lindau, Switzerland; I. Christl, G. Furrer, R. Hindshaw, M. Kiczka, R. Kretzschmar, E. Lemarchand, J.G. Wiederhold, J. Zeyer, Inst. of Biogeochemistry and Pollutant Dynamics, ETH Zürich, Universitätstrasse 16, 8092 Zürich Switzerland; N. Derungs, E.A.D. Mitchell, WSL Swiss Federal Inst. for Forest, Snow, and Landscape Res., Ecosystem Boundaries Res. Unit, Station 2, 1015 Lausanne, Switzerland; N. Derungs, E.A.D. Mitchell, Lab. of Soil Biology, Inst. of Biology, Univ. of Neuchâtel, 2009 Neuchâtel, Switzerland; P. Edwards, H. Göransson, H. Olde Venterink, Inst. of Integrative Biology, ETH Zürich, Universitätstrasse 16, 8092 Zürich Switzerland; I. Hajdas, S. Ivy-Ochs, L. Wacker, Lab. of Ion Beam Physics, ETH Zürich, Schafmattstrasse 20 CH-8093 Zürich, Switzerland; T. Jonas, J. Magnusson, Snow Hydrology, WSL Inst. for Snow and Avalanche Res, SLF Flüelastr. 11, 7260 Davos Dorf, Switzerland; E.A.D. Mitchell, Lab, des Systèmes Écologiques, EPFL, Station 2, 1015 Lausanne, Switzerland; M. Plötze, Inst. for Geotechnical Eng,, ETH Zürich, Schafmattstr. 6, 8092 Zürich Switzerland; M. Stähli, Mountain Hydrology and Torrents, WSL Swiss Federal Inst. for Forest, Snow and Landscape Res,, Zürcherstrasse 111, 8903 Birmensdorf, Switzerland. *Corresponding author (Stefano.bernasconi@erdw.ethz.ch).

The study of chronosequences has a long tradition, and both ecologists and soil scientists have used the concept of substituting space for time to understand ecosystem and soil evolution (for recent reviews see Walker and del Moral, 2003 and Walker et al., 2010). Receding glaciers progressively expose fresh rock to surface conditions and thus offer an excellent opportunity to study the evolution of ecosystems through time. There is abundant literature on deglaciation chronosequences (Anderson et al., 2000; Baumler et al., 1997; Becker and Dierschke, 2005; Bormann and Sidle, 1990; Doblas-Miranda et al., 2008; Dolezal et al., 2008; Egli et al., 2010; Fastie, 1995; Schmidt et al., 2008), but soil and ecosystem development in glacier forefields have so far been analyzed and described mainly from a monodisciplinary perspective (e.g., mineralogy, soil chemistry, microbiology, or vegetation succession). These studies have revealed patterns of ecosystem evolution, such as vegetation succession patterns, the evolution of nutrient limitations (Walker et al., 2010), and changes in microbial communities (Nemergut et al., 2007; Jumpponen, 2003; Lazzaro et al., 2009). Similarly, soil scientists have used glacial chronosequences for the understanding of the rates of soil formation and mineralogical changes (Egli et al., 2006; Mavris et al., 2010). However, the functional linkages between rock weathering, buildup of C and N in the soil, and the role of microbes, plants, and their interactions therein are only partly understood. Moreover, recently deglaciated soil chronosequences have been used to better understand and constrain weathering mechanisms and weathering rates (Anderson, 2007). Generally, low temperatures are considered to limit weathering rates, but the creation of fine-grained sediments with highly reactive surfaces could lead to high chemical denudation rates (Anderson, 2007). The role of biological activity in influencing such chemical erosion rates is a matter of debate and requires additional studies.

Many available glacial chronosequences have only a limited temporal extent, typically approximately 150 yr, the time since the last major glacier advance related to the Little Ice Age (LIA), which in the Alps lasted approximately from 1560 to 1850 CE. These chronosequences offer the opportunity to study fundamental processes related to initial ecosystem establishment on a barren substrate, strategies for nutrient acquisition by microorganisms and plants in oligotrophic systems, and mechanisms of soil organic matter accumulation and preservation.

In this paper we describe the approach and first results of the interdisciplinary project "BigLink" (Bernasconi and BigLink project members, 2008; see http://www.cces.ethz.ch/projects/clench/BigLink [verified 8 July 2011]) on the soil chronosequence developed on the forefield of the Damma glacier, Switzerland. One of the key points of our research approach was to study the evolution of the soils from many disciplinary perspectives simultaneously. Thus, we established a network of sites that were sampled according to a common scheme and subsequently analyzed by all groups to ensure comparability of the data. Our first aim was to evaluate whether there are functional linkages between rock weathering, buildup of soil organic matter (SOM), and the density, diversity, and activity of soil microbes and plants, as well as to examine the possible feedback mechanisms. A second aim was to analyze whether abiotic or biotic indicators can be identified which characterize specific states of the soil development. We present an overview of the main characteristics of the Damma glacier forefield and discuss the evolution of the soil and ecosystem during the last 150 yr.

Previous studies on the Damma glacier forefield have mainly concentrated on microbiological aspects (Duc et al., 2009; Frey et al., 2010; Haemmerli et al., 2007; Lazzaro et al., 2009; Schmalenberger and Noll, 2010; Sigler and Zeyer, 2002; Sigler et al., 2002; Brunner et al., 2011) and have mostly focused on the youngest soils. Geochemical studies of the Damma forefield have focused on the isotope geochemistry of strontium (de Souza et al., 2010) and calcium (Hindshaw et al., 2011a) during weathering, as well as iron during uptake by plants and initial soil formation (Kiczka et al., 2010; Kiczka, 2011). In this study we included a larger number of sites, covering the whole chronosequence. In addition to the soil studies, a hydrological, glaciological, and meteorological monitoring program has also been implemented to characterize the water and element fluxes at the watershed scale. Some of the results of the hydrological studies were discussed in Magnusson et al. (2010, 2011) and Hindshaw et al. (2011b).

Study Site and Glacier Retreat History

The research site is located in the Central Alps, in the canton of Uri, Switzerland (46°38′ N 8°27′ E), in front of the Damma glacier at an altitude between 1950 and 2050 m above sea level (Fig. 1). The climate is characterized by a short vegetation period (late June to mid October), and about 2400 mm precipitation per year. The bedrock is composed of a coarse-grained granite of the Aare massif, which was metamorphosed under greenschist facies conditions and is composed of quartz, plagioclase, potassium feldspar, biotite, and muscovite (Schaltegger, 1990). Epidote is present in significant amounts, mainly as inclusion in plagioclase. Additional accessory minerals include magnetite chlorite and apatite. Although different varieties of metagranite, distinguished mainly by variations in the relative mineral proportions and grain size, are present in the catchment, the composition of the bedrock is very similar everywhere along the chronosequence.

The front of the northeast-exposed Damma glacier has retreated at an average rate of approximately 10 m yr^{-1} since the beginning of systematic annual measurements in 1921, culminating in 2003 with the disconnection of a dead-ice body, a large block of stagnant ice detached from the main glacier remaining in the valley. The active glacier currently terminates above a steep wall at the valley head.

The recession of the Damma glacier since the end of the LIA in 1850 has not been continuous, but was reversed during 1920 to

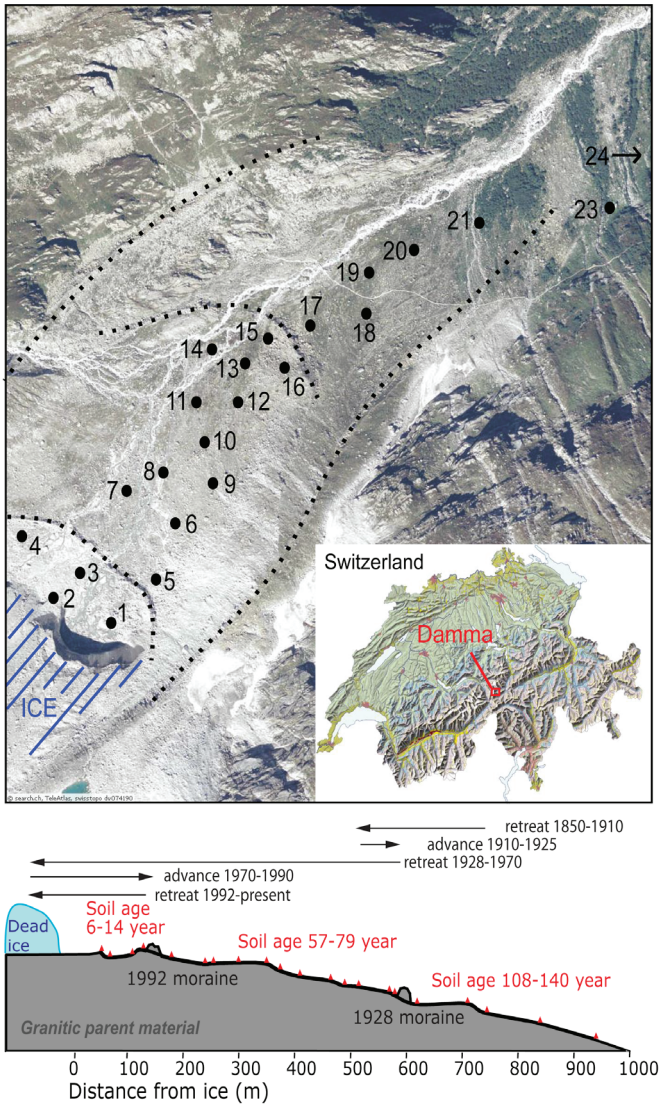

Fig. 1. Location of the sampling sites at the Damma Glacier forefield, with age estimates based on the glacier retreat history.

1928 and 1970 to 1992, resulting in two small terminal moraines clearly visible in the field (Fig. 1). Because of these re-advances the soil chronology is not continuous, but rather consists of three groups of soil ages. We determined the age of the soils on the basis of the measured ice recession history and the presence of moraines in the field. The position of the glacier before the beginning of the measurements in 1921 was estimated through comparison with neighboring glaciers where longer records exist. The length variation data were provided by the Swiss glacier monitoring network operated by the VAW (Versuchsanstalt für Wasserbau, Hydrologie und Glaziologie, http://glaciology.ethz.ch/swiss-glaciers/glaciers/damma.html [verified 8 July 2011]). The youngest sites include soils from 2 to 18 yr old, the intermediate group comprises locations freed from the ice between 1930 and 1950, and the oldest group includes soils that started to form between 1870 and 1897. The soils in between have been eroded during the glacial advances. In addition, we defined two reference sites outside the forefield. These sites lay outside the 1850 LIA moraine and thus were not covered by ice for at least 10,000 yr, and as a consequence no well-constrained age can be assigned to these soils.

Site Selection and Sampling Strategy

One of the main challenges in studying such a proglacial environment is the extreme spatial variability of the system. The glacier forefield is a braided stream system with a main channel, the Damma Reuss, in the center of the valley (Fig. 1) and numerous ephemeral streams on the sides. The position of these streams can change over the years in response to the location of the glacier tongue and seasonally in response to changes in discharge. The valley floor is covered by poorly sorted glacial till ranging in size from fine silt to house-sized boulders. Therefore, it is important to have sufficient replicate sites along the chronosequence to capture the evolution with time and distinguish it from the spatial heterogeneity within soils of any given age caused by the variability of the substrate where soils are forming. In addition, young soils with little vegetation may be strongly influenced by sediment reworking and redeposition, especially during snow melt, and runoff channels in such a system can migrate rapidly. Thus one of the first tasks was to determine a set of sampling sites along the chronosequence that would capture the increase in age and at least some of the heterogeneity of the field. An additional criterion was some degree of randomness to avoid sampling biases. The 21 sites within the chronosequence were selected to cover a range of ages from <10 to about 140 yr by dividing the forefield into a grid. Within this grid, the coordinates were then randomly chosen before visiting the actual locations. The sites were marked, and their GPS coordinates were recorded. Soil ages between the moraines were estimated by measuring the distance between the sampling sites and the dead-ice body, the 1992 moraine, or the 1928 moraine.

A prerequisite for site selection was that the location within the predetermined grid was not visibly disturbed by fresh alluvial material transported by the glacier streams or by avalanches, as that would have altered the soil age. This was relatively easy to recognize at the younger sites, but became harder at older sites that were completely covered by vegetation. The sampling site area was defined as a square of 2 by 2 m, within which three sections of 50 by 50 cm were chosen. We first removed the layer with moss, litter, and pure organic matter and then sampled the mineral soil from 0- to 5-cm and 5- to 10-cm depths. Due to the rocky nature of the soils and the weak soil development at some sites the depths could not always be followed very precisely. Soil sampling was performed in September 2007, and aboveground vegetation was sampled again on new subplots in July 2008, at maximum vegetation growth.

Fig. 2. Pictures of sampling Sites 2, 10, and 17, representative of the three soil age groups, showing the progressive development of the vegetation and soils along the chronosequence.

Description of Individual Sampling Sites

According to the FAO soil classification (IUSS Working Group WRB, 2006) the soils in the forefield can be classified as Dystric Hyperskeletic Leptosols up to and including Site 14 and as Eutric Hyperskeletic Leptosols from Sites 15 to 22. The soils at the two reference sites are Haplic Cambisols (Dystric, Humic, Skeletic). According to U.S. soil taxonomy (Soil Survey Staff, 2010) the soils in the forefield are classified as Typic Cryorthent and the two reference sites as Typic Dystrocryept.

Young Sites (Sites 1–4)

The youngest sites, located between the 1992 moraine and the dead-ice body, became ice-free 6 to 13 yr ago (Fig. 2a). They are characterized by barren rocks, larger boulders, and gravel with sandy-silty sediment between the boulders. Vegetation is scarce and patchy, with mainly mosses, lichens, forbs, and grasses. The dominant plant species are *Agrostis gigantea* Roth, *Rumex scutatus* L., *Cerastium uniflorum* Thom. ex Reichb., and *Oxyria digyna* (L.) Hill. The organic C content of these incipient soils is very low and ranged between 0.1 and 0.4%.

Intermediate Age Sites (Sites 5–16)

The chosen soil sites located between the 1992 and 1928 moraines became ice-free between 1950 and 1930 AD (Fig. 2b). Over this range, vegetation cover increases from partial to full. Dominant plant species are *Agrostis gigantea*, *Salix* spp., *Deschampsia cespitosa* (L.) Roem. & Schult., and *Athyrium alpestre* (Hoppe) Milde. The soils show a better-developed structure, including a litter layer, in comparison to the younger sites. The organic C content in the upper (0–5 cm) mineral soil increases, with some scatter, exponentially as a function of age, from 0.2% to around 2%. There is some heterogeneity with varying distance to the river, for example, in soil moisture, and this is reflected in the vegetation type.

Old Sites (Sites 17–21)

The soil sites below the 1928 moraine originate from the late 19th century (Fig. 2c). Vegetation cover is full and is characterized by woody plants such as *Rhododendron ferrugineum* L. and *Salix* spp., and grasses like *Agrostis gigantea* and *Festuca rubra* L. An exception is Site 21, which has completely different vegetation because it is located in a patch with *Alnus viridis* (Chaix) DC. trees. Soil horizons are clearly visible, and total organic carbon contents (TOC) of the 0- to 5-cm mineral soil vary between 1.2 and 4%. Site 20 is suspected to have experienced secondary deposition of sediments.

Reference Sites (Sites 23 and 24)

Site 23 is located just above and on the outside of the 1850 moraine between a big boulder and a steep wall and is probably not influenced by erosional deposition from above. Site 24 is 0.6 km from the forefield on a relatively flat area and also reasonably shielded from erosional material from the above-lying terrain. Both sites are dominated by the grass *Agrostis gigantea* and ferns. In the topsoils (0–5 cm) TOC contents range around 10%.

Analytical Methods

Soil Sampling and Processing

The soil samples were sieved in the field to <8 mm; stones larger than approximately 8 cm were discarded, and those between 8 mm and 8 cm were weighed and then discarded. In total 3 to 5 kg of field-moist soil was sampled at each site. All samples were brought to the laboratory each evening and stored at 4°C until further processing. From each sampling depth, around 1 kg was dried at 40°C and further sieved into a 2- to 8-mm and a <2-mm fraction, of which the latter was used for most analyses. The dried soils were stored in the dark at 18°C in polyethylene bottles. The remaining wet soil was either used directly for analyses requiring immediate processing, or stored frozen at −15°C.

In 2008, Sites 2, 11, and 19 were sampled again to determine the fractional volume and weight of the <2-mm soil in the forefield

(i.e., kg soil m^{-2} surface cm^{-1} depth) compared to >2-mm material. Four to five holes of approximately 20 by 30 cm were dug, from which the litter layer/root mat was carefully removed, and subsequently upper and lower soil layers were sampled. The emptied volumes were determined by filling them with Lightweight Expanded Clay Aggregate (LECA) balls (Liapor GmbH, Hallendorf, Germany) with a measured density of 360 g L^{-1} and subsequent weighing. Volume taken up by immovable stones was determined by subtracting the measured volume from the volume of the virtually sampled box. All >8-mm material was weighed and discarded, while all <8-mm soil was sampled, taken to the laboratory, and further treated as described above.

Grain Size Analysis

For grain size analysis, organic matter was removed from the soils by treatment with 30% hydrogen peroxide. The carbon-free samples were dried at 105°C and finely ground using a hand mortar. An aliquot was dispersed in a 0.2% Calgon solution and the silt and clay fractions determined using the pipette method by Gee and Bauder (1979). Sand was defined as 2 mm to 63 μm, silt as 63 to 2 μm, and clay as <2 μm.

Mineralogy

The mineralogical composition of the fine sand fraction (63–250 μm) and clay fraction (<2 μm) of 12 selected sites and from representative rock samples was determined with X-ray diffraction analysis using a BRUKER AXS D8 diffractometer with CuKα radiation. Measurements were performed on both randomly oriented specimens and on smear slides for better identification of clay minerals (Brindley and Brown 1980). The mineral phases were identified in comparison to the International Centre for Diffraction Data (ICDD) database with the software package DIFFRACplus (Bruker AXS). The quantitative mineralogical composition was determined using Rietveld analysis (Rietveld, 1969). For a detailed description of the methods see Mavris et al. (2010).

Soil pH

Soil pH was determined both in 0.01 M $CaCl_2$ (soil/solution ratio 1:2, 30-min reaction time under stirring, measurement in stirred suspension using a glass electrode Schott Blue Line 22 pH) and in deionized water (Millipore Milli-Q, soil/solution ratio 1:2.5, 60-min reaction time under shaking, measurement in the supernatant after 120 min without shaking using a glass electrode Metrohm 6.0234.100) at room temperature.

Cation Exchange Capacity, Base Saturation

Soil samples were extracted with 1 M NH_4Cl (soil/solution ratio 1:10) for 1 h at 20°C using a shaker and immediately filtered (Whatman 790 1/2). The metal concentrations in the extracts were measured using inductively coupled plasma optical emission spectrometry (ICP–OES, PerkinElmer Optima 3000). For exchangeable acidity, soil samples were extracted with 1 M KCl (soil/solution ratio 1:10) for 1 h at room temperature on a shaker and immediately filtered (Whatman 790 1/2). Total exchangeable acidity was determined by titration of the extract with NaOH to pH 8.2. Exchangeable Al was complexed with fluoride and measured by back titration with HCl. Exchangeable protons were calculated as the difference between total exchangeable acidity and exchangeable Al. The effective cation exchange capacity (CEC_{eff}) was calculated as sum of exchangeable H^+, Al^{3+}, Na^+, Mg^{2+}, K^+, Ca^{2+}, Mn^{2+}, Fe^{3+}, and Zn^{2+} ($mmol_c\ kg^{-1}$). The base saturation (BS) was calculated as sum of Na^+, Mg^{2+}, K^+, and Ca^{2+} divided by CEC_{eff} (%).

Chemical Composition of Soils

The inorganic chemical composition of the soils was determined by ICP–OES after a total digest procedure for the lightest elements (Na, Mg, K, and Ca) and by X-ray fluorescence spectroscopy (XRF) for other elements. For total digest, a few grams of the <2-mm dried soil fraction were crushed in a tungsten carbide mill to obtain a fine powder. One hundred milligrams of this powder was introduced in a Teflon bomb reactor, and an acid mixture was added (0.5 mL HF_{conc} + 1 mL HNO_{3conc} + 2 mL HCl_{conc}). The reactor was left overnight at room temperature and then heated at 150°C for 1 h in a microwave oven. The solution was then evaporated to dryness on a hotplate, and the solid was redissolved in 10 mL of HNO_3 (7 N). In addition, the <2-μm fraction of four soils (Site 2, 0–5 cm; Sites 15, 18, and 24, 5–10 cm) were digested by the same procedure, and the concentrations of major elements were also measured using ICP–OES. For XRF measurements, 4 g of the <2-mm dried soil fraction were crushed in a tungsten carbide mill, mixed with 0.9 g of Licowax C Micropowder PM (Fluxona), and pressed at 1.5 t cm^{-2} to form the pellets that were then analyzed. The XRF instrument was calibrated using the international standards BCR-2, LSKD-1, SO-1, SO-3, SO-4, SS-1, SS-2 using the analytical values listed in the GeoReM database (http://georem.mpch-mainz.gwdg.de/ [verified 11 July 2011]).

Total Organic Carbon and Nitrogen Contents

For elemental analysis soils were finely powdered in a disk mill and measured with a FlashEA 1112 elemental analyzer, calibrated with Atropin (70.56% C, 4.84% N) and two soil reference samples Soil 1 (3.5% C, 0.216% N) and Soil 5 (0.141% C, 0.021% N) distributed by HEKAtech (Wegberg, Germany). Analytical reproducibility is better than 0.2% for soils with a C content above 1% (w/w) and increasing to 3% for very low-C soils. The reproducibility of the N content was typically 5% for soils with more than 0.1% N (w/w), but deteriorated for very low N samples.

Microbial Carbon, Nitrogen, and Phosphorus

Microbial C and N were determined by the fumigation–extraction method of Vance et al. (1987) and microbial P by liquid fumigation with hexanol and extraction of P with anion exchange resin membranes (Kouno et al., 1995). All microbial biomass values are reported as the difference between fumigated and nonfumigated subsamples, without the use of a conversion factor. Phosphorus extracted from nonfumigated subsamples is presented as available P (P_{resin}).

Vegetation

In September 2007, vegetation composition was recorded on 49 m^2 in every plot, using the Braun–Blanquet scale. Additionally, the vegetation was cut just above the moss/litter layer. In the laboratory it was divided into woody and green tissues, dried at 40°C for 5 d, and weighed. To estimate the vegetation biomass per square meter, the vegetation cover in each subplot was estimated using photographs taken in 2008 from approximately 4-m height and covering 25 m^2 each. The average vegetation biomass per square meter was calculated by combining the biomass weight determined from the small subplots sampled in 2008 with the vegetation cover determined by image analysis.

Soil Sampling for Microbial Studies

Soils were sampled with an ethanol-sterilized shovel, placed into 50-mL Falcon tubes, and stored in a cool box. After sieving through a 2-mm grid and manual removal of fine roots in the laboratory, the soil samples were stored in new Falcon tubes at −80°C until analysis.

Nucleic Acid Extraction

Total nucleic acids of frozen soil samples were extracted with the Smart Helix DNA extraction kit (Venturia, Ljubljana, Slovenia) according to the manufacturer's recommendations. Extractions were performed in triplicates from all samples. The extracted DNA was dissolved in 40 μL of AE-Buffer and stored at −20°C until use. DNA content was quantified using PicoGreen (Invitrogen, Carlsbad, CA).

Polymerase Chain Reaction and Terminal Restriction Fragment Length Polymorphism Analysis

For specific polymerase chain reaction (PCR) amplification of bacterial 16S rRNA genes, the primers 27F (FAM-labeled) and 1378R were employed (Heuer et al., 1997). For specific amplification of fungal 18S rRNA, the primers nu-SSU0817 (FAM-labeled) and nu-SSU1536 were used (Borneman and Hartin, 2000). Five to two hundred nanograms of DNA were added as a template for the PCR reactions of the bacterial 16S rRNA and fungal 18S rRNA; PCR conditions were similar, as previously described (Borneman and Hartin, 2000; Frey et al., 2006). PCR products were digested with either the restriction enzyme *Msp*I for bacteria or *Alu*I for fungi. The primers were obtained from Microsynth AG (Balgach, Switzerland), and the enzymes were from Catalys (Wallisellen, Switzerland). Terminal restriction fragment length polymorphism (T-RFLP) analyses were performed on an ABI Prism 310 Genetic Analyzer (Applied Biosystems, Carlsbad, CA), and the T-RFLP profiles were analyzed using Genotyper v.3.7 NT (Applied Biosystems) according to Frey et al. (2006). The Shannon diversity index (H) was calculated according to the formula:

$$H' = -_n\Sigma^{ni}[(n_i/N)\ln(n_i/N)] \quad [1]$$

where N is the sum of all peaks, and n_i is the peak height (Sigler and Zeyer, 2002).

Phospholipid Fatty Acids Analyses

Samples from the 0- to 5-cm soil depth, sieved through a 2-mm sieve and freeze-dried, were extracted with a chloroform–methanol–citrate buffer (0.15 M, pH 4.0) (1:2:0.8 v/v/v) according to Frostegard et al. (1991). Each sample was spiked with 300 μg of heneicosanoic fatty acid (C21:0, H5149, Sigma-Aldrich, Buchs, Switzerland) as internal standard. Phospholipids were isolated by silica gel column chromatography (Kates, 1986), transesterified into phospholipid fatty acids (PLFA) methyl esters (Poerschmann and Carlson, 2006) and analyzed by gas chromatography. Fatty acids were identified by comparing their retention times with those of several commercial standards and further confirmed by gas chromatography–mass spectrometry at the Institute of Organic Agriculture (FiBL, Frick, Switzerland). We used the C18:2ω6,9c fatty acid as biomarker for soil fungi, and the sum of C15:0, C16:1ω7c, C17:0, and C18:1ω7c as biomarker for soil bacteria (Frostegard and Baath, 1996).

Testate Amoebae

Testate amoebae were selected among soil organisms because of their role in mineralizing nutrients and regulating bacterial populations and their ease of observation by light microscopy (Mitchell et al., 2008; Wilkinson 2008). The shell (test) they produce, which has diagnostic value to species level, is preserved after the death of the organism. Testate amoebae are therefore a good group of model organisms to study ecological gradients and succession (Carlson et al., 2010). Testate amoebae were extracted from the <2-mm soil fraction (1–5 g dry weight depending on the samples). The soil samples were placed in a 50-mL centrifugation tube with approximately 30 mL of deionized water. The tubes were shaken for 1 min to disaggregate the soil and to separate the amoebae from the soil particles. The solution was then filtered through a 200-μm mesh filter to remove large particles. *Lycopodium* spore tablets were added to the samples for absolute counts (batch no 938934, x = 10679 spores/tablet, one tablet added per sample) (Stockmarr, 1971). The *Lycopodium* spores were counted along with testate amoebae. We aimed to reach a minimum of 150 individuals counted per sample. In five samples with low density this total was reduced to 100 individuals. In two other samples the density was extremely low, and only very few (i.e., 6 and 9, respectively) testate amoebae could be found even after a counting period of approximately 6 h. Living and dead (empty shells) testate amoebae were counted separately. However, species richness, density, Shannon diversity (Shannon–Wiener index) and evenness (Hill) were calculated based on the total of living plus dead individuals to make use of all available data. Evenness was calculated as the Hill's ratio of Shannon's diversity to species richness (Hill, 1973).

Statistical Analysis

To address the question of whether the different sites cluster in their T-RFLP patterns representing bacterial and fungal communities in the soil, a cluster analysis was performed in STATISTICA (StatSoft, Tulsa, OK). Principle component analysis (PCA)

and redundancy analysis (RDA) of selected variables describing the soil and ecosystem properties along the chronosequence were performed using the software package CANOCO v. 4.5 (Microcomputer Power, Ithaca, NY). This was done to examine the relationship between the different parameters and groups of parameters. The age (time from deglaciation) and the distance from ice for the two reference sites were not specified. Each column of the dataset was centered and standardized to make the variables comparable between each other. The RDA was used to test the importance of several key factors for explanation of the trends in the other variables. To this end, six factors were specified (soil age, distance from glacier, C content, plant biomass, and elevation) and used to overlay the resting variables regarded as independent explanatory dataset. The model was tested with Monte-Carlo permutation test (9999 permutations, full model).

Results

Soil Physical and Chemical Characteristics

Soil Mineralogy and Soil Texture

The mineralogy of the soils reflects the homogeneous composition of the bedrock in the glacier forefield and is composed of quartz, plagioclase, potassium feldspar, biotite, muscovite, and epidote with minor apatite. The surface soil texture (0–5 cm) ranged from silty sands within the chronosequence to loamy sands at Sites 23 and 24 (Fig. 3). The deeper (5–10 cm) mineral soils were mostly silty sands, except at Site 15, where it was sand. The clay content exhibited a weak tendency to increase with age in the 0- to 5-cm layer (Fig. 3), and silt showed a weak tendency to increase with age in the subsoil (data not shown). Quartz tends to be enriched in the sand fraction and biotite, muscovite, and chlorite in the <2-μm fraction. Feldspar (particularly plagioclase) is slightly depleted in the clay fraction compared to the sand fraction, whereas the silt fraction is enriched in epidote.

There are only minor mineralogical differences between the 0- to 5- and 5- to 10-cm layers. With increasing soil age, a decreasing albite content is observed (Table 1). Soils older than 110 yr (Sites 17–24) show the formation of secondary chlorites (hydroxy-interlayered vermiculites) found particularly in the clay fraction (Table 1). Only the reference Site 24 shows a small amount of kaolinite in the <2-μm fraction (data not shown).

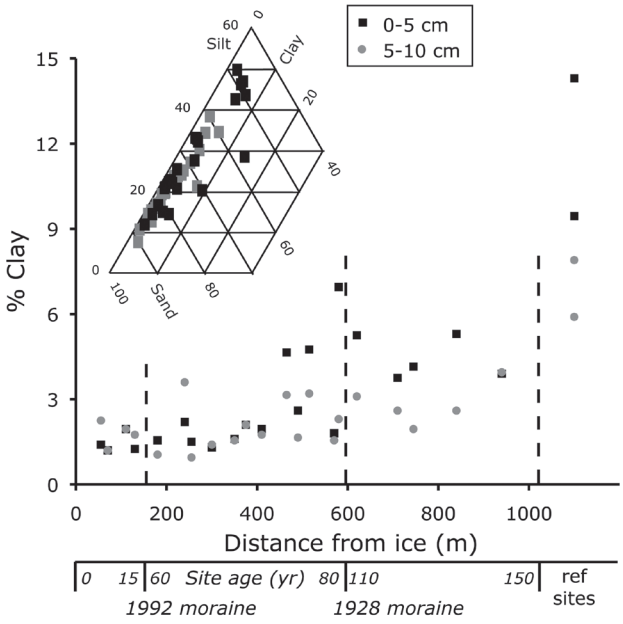

Fig. 3. Clay content of soils along the chronosequence, showing an increase in the oldest soils. The inset shows the grain size distribution in a ternary diagram sand–silt and clay.

pH, Cation Exchange Capacity, Base Saturation

Soil pH was determined in 0.01 M $CaCl_2$ and additionally in deionized water, as the soil solution in these soils is very dilute. Typically, the pH value measured in deionized water was about 0.4 to 1.0 pH units higher then in 0.01 M $CaCl_2$. The pH values of the 0- to 5- and 5- to 10-cm layers decreased along the chronosequence from 5.5 to 3.6 when measured in 0.01 M $CaCl_2$ and from 6.2 to 4.0 in deionized water (Fig. 4). In most soils, the 0- to 5-cm layer exhibited a significantly lower pH value than the 5- to 10-cm layer. The soils at Sites 12, 15, and 20 deviated from this behavior and exhibited a higher pH than expected from their location in the chronosequence.

The CEC_{eff} increased, and the BS decreased with age (Fig. 5A, 5B). The soils at Sites 12, 15, and 20, however, exhibited an exceptionally high BS for their location in the chronosequence. At the older sites, both CEC and BS in the 0- to 5-cm layer were distinctly higher than in the 5- to 10-cm layer. Sites 12, 15, and 20 share relatively high

Table 1. Average mineralogy of the fine sand, silt and clay fractions of the soils in the forefield averaged by age groups.

Soil age group	K-feldspar			Albite			Biotite			Muscovite			Epidote			Chlorite and Hydroxy-Interlayered Vermiculites		
	Fine sand	Silt	Clay	Fine sand	Silt	Clay	Fine sand	Silt	Clay	Fine sand	Silt	Clay	Fine sand	Silt	Clay	Fine sand	Silt	Clay
	%																	
Young	12.5	11.3	12.5	24.3	24.3	30.4	1.4	7.6	13.4	3.0	15.9	18.4	2.5	5.2	3.9	0.6	3.0	11.1
Intermediate	11.0	10.5	11.2	26.2	28.0	24.5	1.7	6.8	19.6	3.0	15.9	20.1	2.7	6.9	2.4	0.7	2.7	13.6
Old	11.7	10.9	11.0	28.3	28.8	20.9	1.4	4.0	14.0	3.8	12.0	18.0	3.6	7.1	3.1	0.6	6.8	24.6
Reference sites	8.8	6.8	4.6	31.7	21.6	7.0	0.9	3.7	4.7	5.0	22.2	19.6	4.1	6.7	0.6	1.2	18.3	49.5

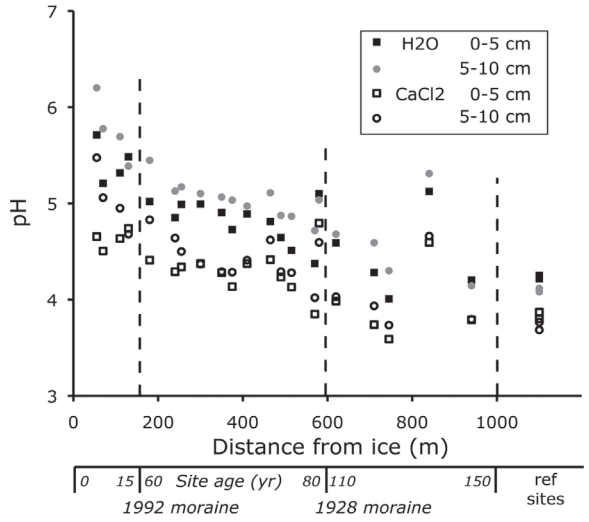

Fig. 4. Evolution of pH in the topsoil (0–5 cm) and the subsoil (5–10 cm) along the chronosequence as measured in deionized water and 0.01 M $CaCl_2$. Vertical lines indicate the position of the moraines from 1992 and 1928.

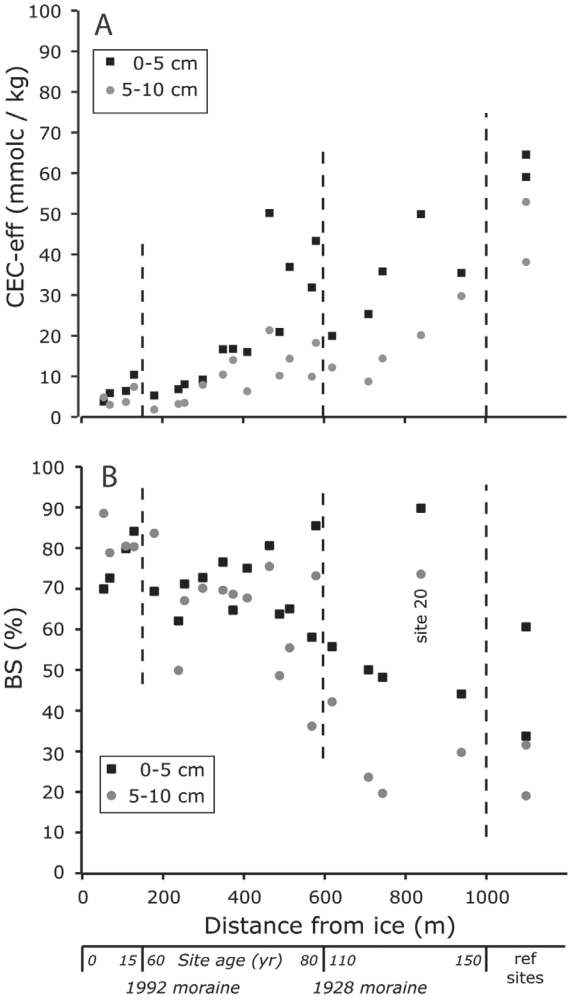

Fig. 5. (A) Cation exchange capacity and (B) base saturation in the top- and subsoil along the chronosequence.

CEC, BS, and pH values (Fig. 4 and 5). We attribute this anomaly to the fact that these sites are much wetter than the others because of groundwater seepage to the surface and to the higher clay contents of 7, 5.3, and 5.3%, compared to the average of 3.5% (Table 1). In addition, Site 20 may have been affected by recent sediment depositions.

Major and Trace Element Chemistry of Soils

Most elements do not show any or only minor concentration trends along the soil chronosequence, except for the two reference sites, Sites 23 and 24. Representative soil analyses are reported in the supplementary information. The chemical index of alteration, defined as the ratio of aluminum to the sum of the major cations, {CIA = [Al]/([Al] + [Na] + [K] + [Ca] + [Mg])} (Fig. 6) scatters between 0.55 and 0.65 and for all soils along the chronosequence is very close to that calculated for the fresh parent rock (0.55), showing a small degree of weathering of the mineral matrix of these soils. Even in the finest fraction (<2 μm), the CIA increases significantly only for the oldest reference site, to a value of 0.74. Thus, in agreement with the mineralogical data, at all sites the fine fraction is mainly a product of mechanical erosion rather than of secondary chemical weathering of minerals.

Despite the small degree of weathering in the soils, some trends can be observed for a few trace elements. The concentrations of Cl, S, Br, Cu, and Pb increase with soil age, particularly in the 0- to 5-cm layer (data not shown). This could be related to atmospheric deposition. The good correlation observed between the total C contents and these elements, particularly for S and Br, suggest that these elements are complexed by the organic matter formed during pedogenesis or that they are incorporated into the living biomass. Other groups with significant correlation coefficients but without

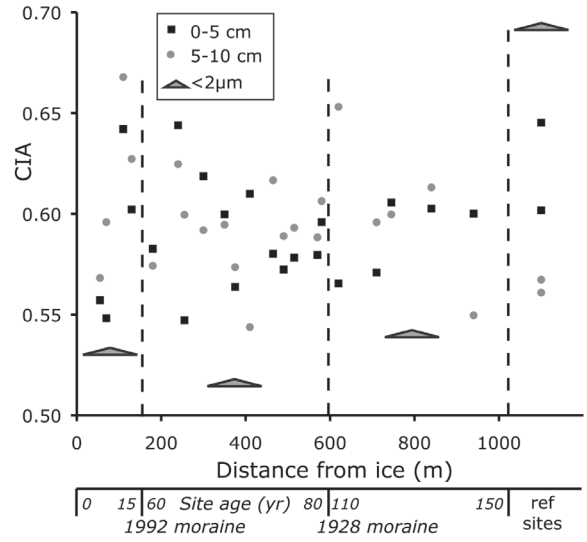

Fig. 6. Chemical index of alteration (CIA) for the bulk soils and the <2-μm fraction, showing small variability along the chronosequence. A clear increase is only observed for the clay fraction in the two reference soils outside the forefield.

clear temporal trends can be distinguished, but these variations predominantly reflect variations in mineral composition of the parent rock rather than the time elapsed since deglaciation.

Soil Organic Matter

Total organic C (TOC) and total N (TN) contents increase exponentially with soil age in the two younger age groups (Fig. 7) and also increases somewhat in the oldest age group, when Sites 20 and 21 are removed from the analysis. The vegetation of Site 21 is completely different as compared to the other sites (*Alnus* trees vs. grass–shrubs), while Site 20 is suspected to have experienced secondary deposition of sediments, and hence may in reality be a younger soil. Remarkably, the TOC content appears to have been "reset" to low values during the re-advance of the glacier: soils just below the moraines contain much less organic matter than could be expected from the age–TOC correlation from the above-lying sites. In addition, the rate of SOM accumulation shows a decreasing trend from the young to the old sites (i.e., on the longer time scale a leveling off of the accumulation rate is observed). The C/N atomic ratios vary between 12 and 30, with no significant trend across the chronosequence. The 0- to 5-cm layers have lower or similar C/N ratios than the subsoil (data not shown).

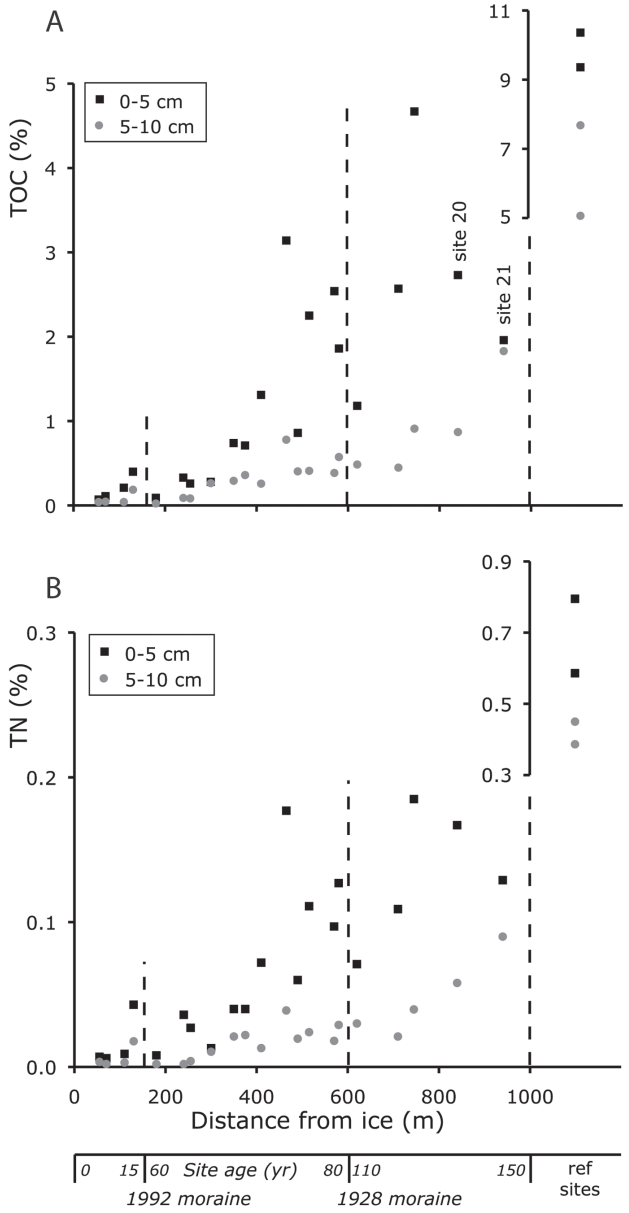

Fig. 7. Total organic carbon (TOC) and total nitrogen (TN) concentrations with age.

Vegetation Succession Along the Chronosequence

Bare soil (soils free of aboveground vegetation) between the stones decreases from more than 90% to less than 10% in less than 70 yr of soil formation, and the aboveground biomass of plants shows a clear increasing tendency with soil age. Total biomass seems to have reached a steady state comparable to the reference sites outside the forefield below the 1928 moraine (Fig. 8A), with the exception of Site 21, which is dominated by *Alnus* spp. trees and thus has a much larger biomass, and Site 12, which is covered mainly by willows (*Salix* spp.). There is a

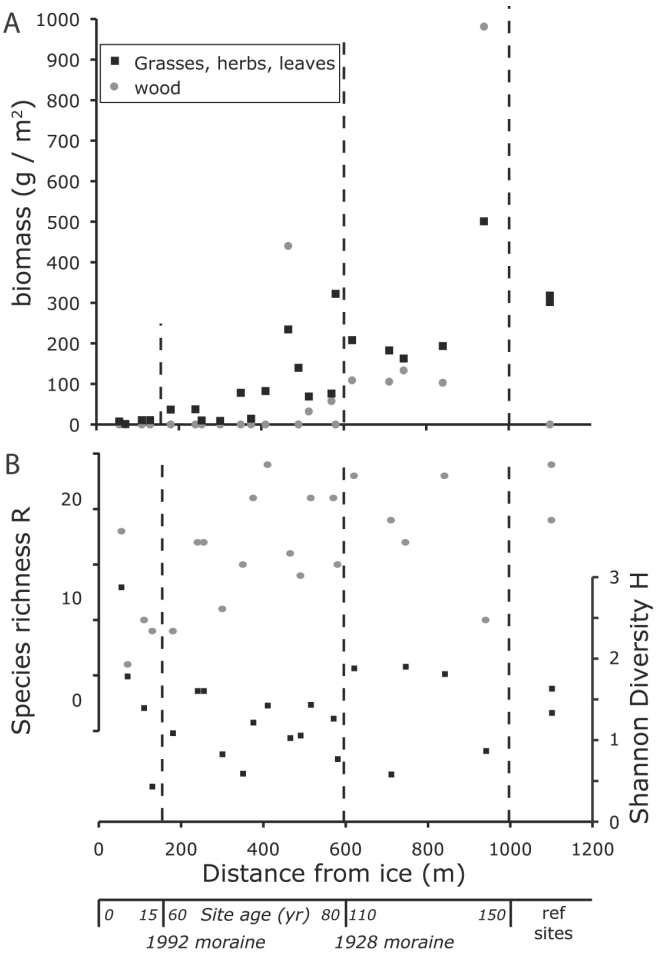

Fig. 8. (A) Aboveground biomass and (B) species richness (dots) and the Shannon diversity index (squares) of plant communities along the chronosequence.

clear vegetation succession, with pioneer forbs dominating the vegetation only at the very young sites, grasses dominating up to about 70 to 80 yr after deglaciation, and woody shrubs (*Rhododendron, Salix* spp.) or tall *Alnus* spp. shrubs dominant at the older sites. The reference sites outside the forefield are dominated by herbaceous plants (grasses, ferns); woody plants are absent. Species richness of plants increases with age, but not the Shannon diversity index (Fig. 8B).

Genetic Profiling of Bacterial and Fungal Communities

DNA concentrations varied between 0.9 and 19.4 μg DNA g^{-1} dry soil (Fig. 9A), and in general the extracted DNA concentrations increased with distance from the glacier terminus. For bacteria, terminal restriction fragment (T-RF) lengths ranged from 50 to 500 relative migration units (rmus). The highest numbers of T-RFs were 96 and the lowest numbers were 36 (data not shown). Two relative migration units are obvious, with the dominant peaks exceeding 5% of the total peak height; one is the region from 84 to 93 rmus and the other from 137 to 152 rmus. In general, T-RFs obtained from older soils were more dominant than the ones from the younger soils. The Shannon diversity index (*H*) of T-RFLP profiles varied between 2.3 and 3.9 (Fig. 9B). *H* slightly decreased with increasing distance from the glacier. Cluster analysis of the T-RFLP data revealed four main clusters (Fig. 10A). Cluster I, encompassing the oldest sites, and Cluster IIa, representing the youngest sites, were separated from the others. Consequently, the youngest and the oldest sites were clearly separated from each other indicating a shift in the bacterial community structures along the chronosequence. The other branch (Cluster IIb) is divided into two branches (Clusters IIIa and IIIb) consisting of intermediate sites only (Cluster IIIb) or mixed soil ages (Cluster IIIa).

Fungal community profiles were determined by using genetic profiling with T-RFLP of the 18S rRNA gene. The numbers of fungal T-RFs was in the range of 2 and 12 per sample and thus were considerably lower than the numbers of bacterial T-RFs detected per sample (data not shown). Dominant T-RFs for *AluI* were in the region from 446 to 450 rmus, exceeding the share of 20% of the total peak height. These T-RFs occurred in almost all samples. The other T-RFs did not exceed 20% of the total peak height. *H* ranged from 0.3 to 1.2 (Fig. 9A). Overall, there was no clear pattern of fungal diversity as indicated

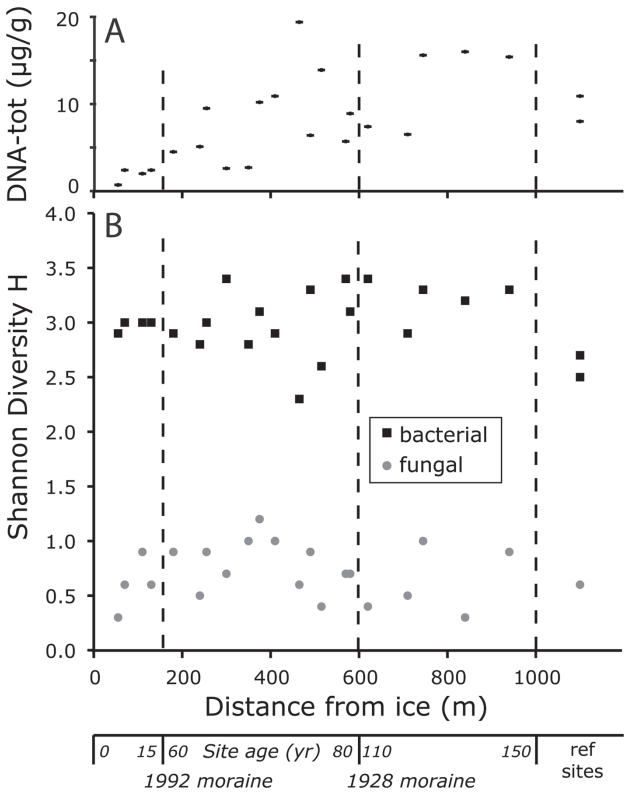

Fig. 9. (A) Total DNA concentrations in soil and (B) Shannon diversity index of bacterial and fungal T-RFLP profiles along the Damma chronosequence.

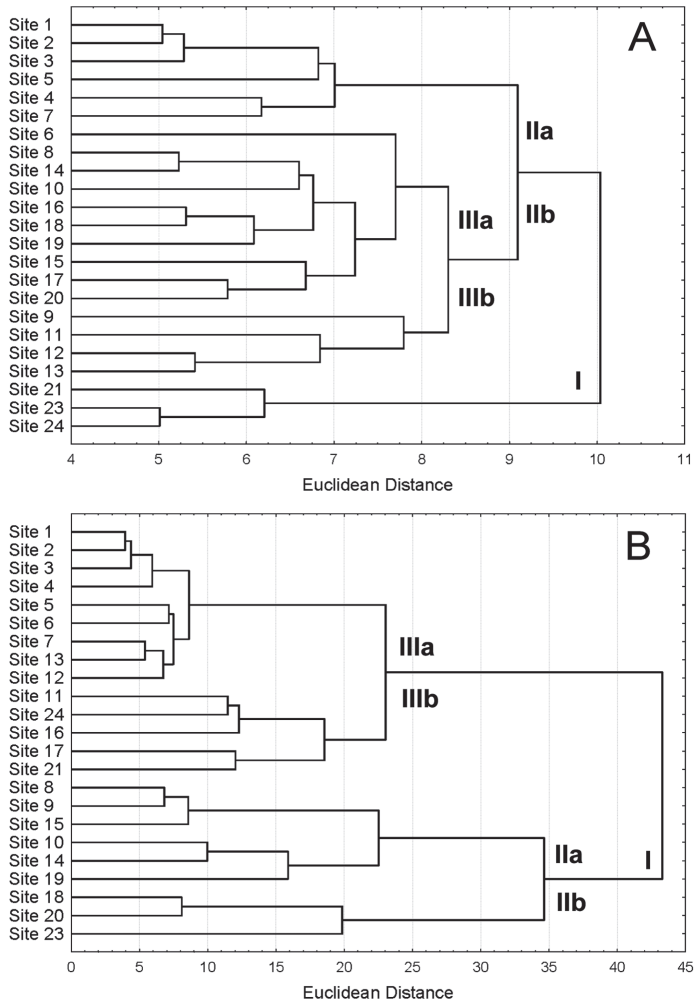

Fig. 10. Cluster analysis of the (A) bacterial and (B) fungal T-RFLP data. Main clusters are marked with roman numerals. The young sites were clearly separated from the old sites (for bacteria: Cluster IIa versus I and for fungi: Cluster IIIa versus cluster IIb).

by the *H* index across the soil chronosequence. Cluster analysis of the T-RFLP data revealed that also for fungal communities, the younger soils (Cluster IIIa) were clearly separated from older soils (Cluster IIb; Fig. 10B). T-RFLP profiles of the intermediate soils were included in the Clusters IIa and IIIb. Shifts in fungal community structures along the chronosequence were clearer than those in bacterial communities, as indicated by the higher Euclidean distances in the cluster analysis for fungal T-RFLP profiles.

Microbial Biomass and Phospholipid Fatty Acids

Microbial C at 0- to 5-cm depth increased from low values of 4 to 30 mg C kg^{-1} in the very young sites to maximum of 102 and 158 mg C kg^{-1} in the intermediate and old sites, respectively (Fig. 11A). In the reference sites, four times higher values were found. Similar trends were observed for microbial N (0.7–161 mg N kg^{-1}) and microbial P (0.1–55.5 mg P kg^{-1}) (data not shown). The 5- to 10-cm soil layer reflected the same increase with site age, but the values were generally 50 to 80% lower than in the 0- to 5-cm soil layer.

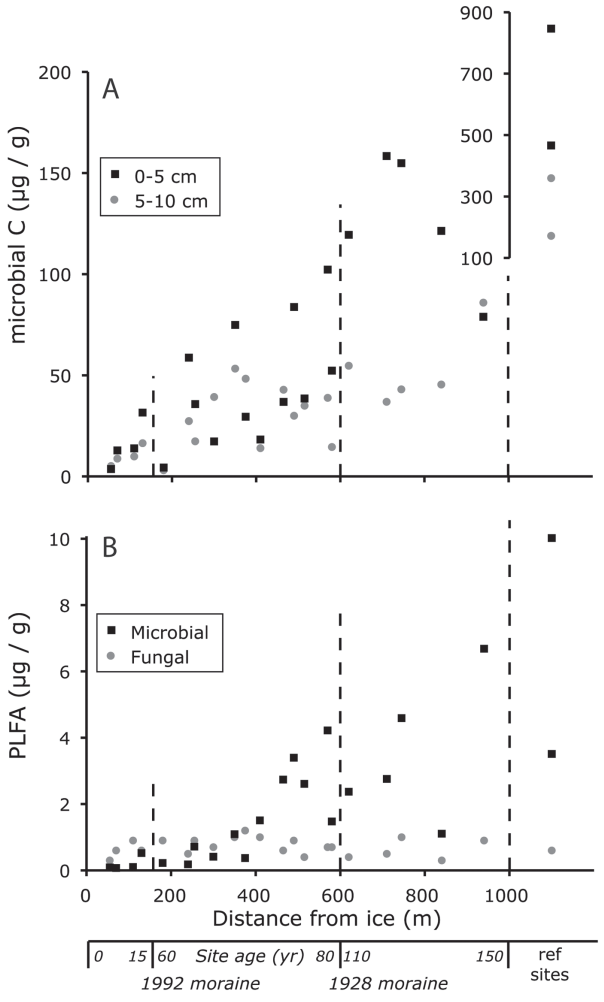

Fig. 11. (A) Microbial C in soils determined with the fumigation method and (B) bacterial and fungal biomass derived from phospholipid fatty acids (PLFA) concentrations.

The concentrations of specific phospholipid fatty acids for both the fungi and bacteria increase along the soil chronosequence (Fig. 11B). The regression analysis excluded the reference sites. Analogous to its effect on TOC, the repeated advance and retreat of the glacier appears to have erased the previous signatures of the soil microbial activity, producing a pattern similar to that observed for soil C (Fig. 8a). The absolute concentrations of fatty acids increase with soil age, but if normalized to organic C, no trend can be observed (data not shown).

Testate Amoebae

Overall the density, species richness, and diversity of testate amoeba communities increased over the chronosequence (Fig. 12). However, diversity expressed as the Shannon index declined in the oldest Sites owing to the strong dominance of some taxa in the community. Evenness was by contrast highest in the younger sites. Density was lower at Sites 1 through 10 compared with the older sites. Samples 15 and to a lesser extent 10 stand out as having much higher density than other sites. Site 15 is close to the river and also stands out by having a high pH, sand content, and clay content and being relatively wet.

Multivariate Statistical Analysis

Principal component analysis performed with many of the abiotic and biotic variables for the 0- to 5-cm soil samples resulted in a strong first axis, explaining more than 40% of the dataset variability (Fig. 13A). This axis is mostly explained by the changes in C concentrations in the soil and closely relates to trends in increasing clay content, available P (P_{resin}), and pools of C, N, and P in the microbial biomass. Some of these variables show very close correlations between each other (e.g., clay content-available soil P and P in microbial biomass, Fig. 13A). This axis also covers trends in bacterial diversity (as assessed by number of T-RFLP) and K/Ti, Fe/Ti,

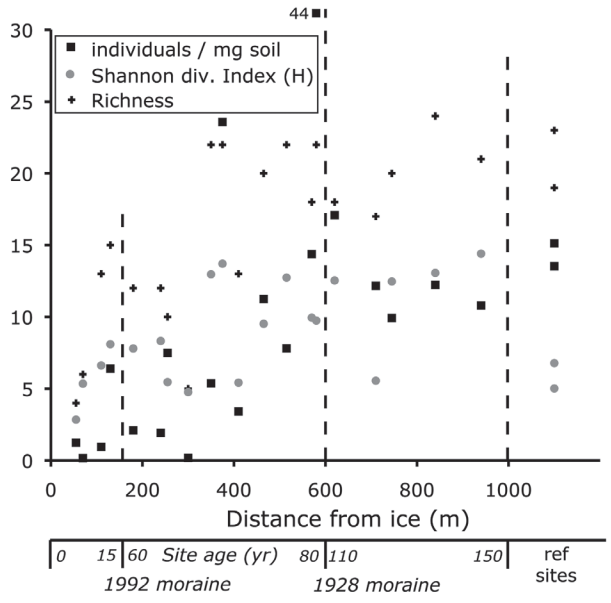

Fig. 12. Abundance, richness, and Shannon diversity index of testate amoebae communities along the chronosequence.

and Mg/Ti ratios of the soil (pointing in the other direction than C increase). Comparing the PCA analyses including (Fig. 13A) and excluding the reference sites (Fig. 13B) it becomes obvious that including the reference sites in the analyses greatly affects the emerging conclusions. The sites from within the forefield obviously form a rather uniform group, which is quite different from the reference sites, and the reference sites greatly extend the length of several of the environmental gradients (Fig. 13A).

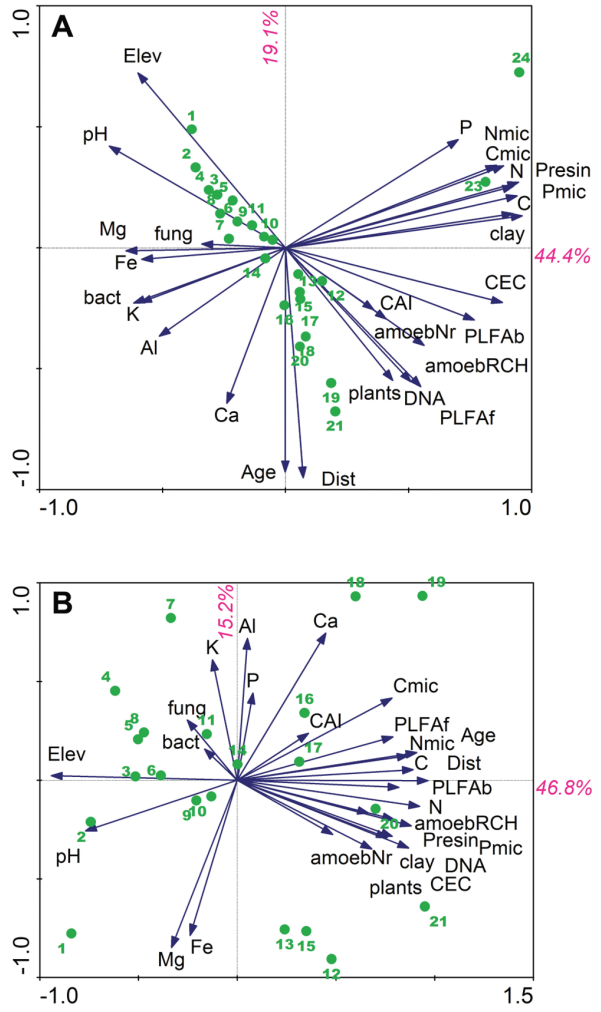

Fig. 13. Principal component analysis (PCA) of selected variables (A) including or (B) excluding the two reference sites. First and second PCA axes are shown, with the proportions of dataset variability explained by each of the axes shown in pink. Sizes of and angles between the vectors representing different variables, and between vectors and the axes, indicate strength of correlation between them and with the PCA axes, respectively. Projections of the sampling sites to the first two dimension of the multidimensional data space are shown in green. Detailed description of the variables and the data are provided in the supplementary data available online. The variables used are: distance to the glacier (Dist), site elevation (Elev), age from deglaciation (Age) soil pH (pH), clay content (clay), elemental composition (C, N, P, Fe, Ca, Al, K, Mg), available P in the soil (Presin), cation exchange capacity (CEC), and chemical alteration index (CAI), diversity of soil bacterial and fungi (bact and fung, respectively), elements in microbial biomass (Cmic, Nmic, and Pmic), plant biomass per unit of soil surface (plant), concentrations of bacterial and fungal PLFAs (PLFAb and PLFAf, respectively), DNA amount per unit soil weight (DNA), amoeba individuals per unit soil weight (amoebNr), and amoeba species richness per site (amoebRCH).

When analyzing the sites within the forefield chronosequence only thus excluding the reference sites (Fig. 13B), soil C remains one of the most important factors determining the positioning of the sampling sites along the first PCA axis, together with site soil age, distance from the ice, site elevation, and soil pH, the last two pointing to the opposite direction of the soil C (Fig. 13B). In this analysis soil C is also closely related to the microbial nutrient pools and the abundance of fungi and bacteria (as assessed

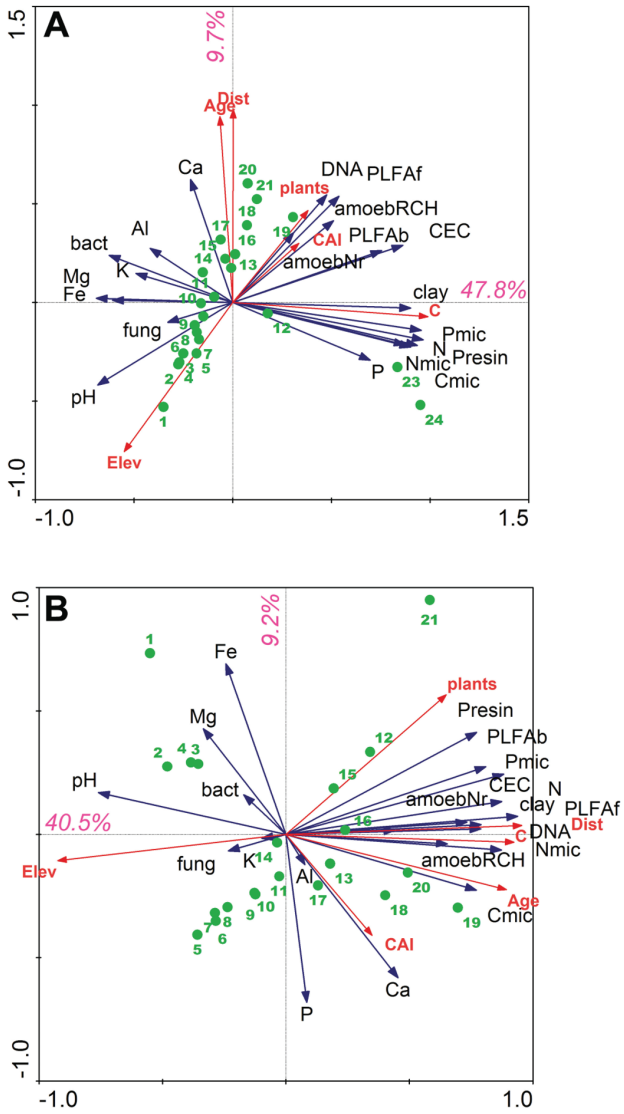

Fig. 14. RDA testing importance of six explanatory variables (C in soil, plant biomass, distance from glacier, age of soil, elevation, and chemical alteration index), shown in red, on array of other measured variables, shown in blue, (A) including or (B) excluding the two reference sites. Monte-Carlo permutation test indicated strong relationships between the set of explanatory variables and the other measured variables ($p < 0.001$ on including or excluding the reference sites). Variable abbreviations as in Fig. 13.

by phospholipid fatty acid markers) and amoebas in the soils. However, soil elemental composition and both bacterial and fungal community diversities all have much lower influence on the distribution of the sampling sites along the first PCA axis than if the reference sites were included (compare Fig. 13A and 13B).

The RDA analyses presented in Fig. 14 illustrate again a strong influence of soil C and (to a lesser extent) of site elevation on the explanation of the entire dataset variability, with the picture being very much driven by the reference sites if those were included (Fig. 14A). If the reference sites were removed from the RDA analysis (Fig. 14B), soil C was closely correlated with soil age and distance from the glacier, as well as (strongly negatively correlated) with site elevation, unlike when the reference sites were retained in the analysis (Fig. 14A). Plant biomass per unit of surface and the chemical index of alteration could not be unequivocally tied down to any of the first two RDA axes (Fig. 14B), indicating that these variables were likely less important factors affecting site properties as compared to soil C.

The above observations were further tested by RDA analyses scrutinizing the effects of the six single explanatory variables (identical to those in Fig. 14) on explaining the variability of the remaining dataset. Upon including reference sites to the RDA, the soil C was the only single variable strongly explaining the data ($p < 0.001$), and only one more factor (site elevation) was contributing significantly to the dataset variability explanation ($p < 0.01$). When excluding the reference sites from the RDA, five single variables (soil C, site elevation, soil age, distance from glacier, and plant biomass per unit surface) all significantly explained the variability in the dataset ($p < 0.001$), whereas only the chemical alteration index of the soil had no significant impact ($p = 0.16$).

Discussion

Soil Physical and Chemical Properties

The mineralogical and inorganic chemical data presented above clearly indicate that soils in the Damma glacier forefield have undergone a small degree of chemical weathering during 150 yr. This is indicated by the relatively constant mineralogy of the <2-μm fraction of younger samples within the chronosequence (<80 yr) and the small variations in CIA. The small increase in clay content observed with age is dominantly a reflection of stabilization of the fine fraction by the vegetation rather than in situ weathering and mineral formation processes, as in the first two soil age groups there is no evidence for clay mineral formation (Table 1). Hydrodynamic sorting is the main cause of the comparatively higher silt content at Sites 10, 12, 13, 15, and 17. Only older soils (>100 yr) show a decreasing albite content with coincidental formation of small amounts of secondary chlorites (Table 1). Only in reference Site 24, was kaolinite observed, forming 7% of the clay mineral fraction. Kiczka et al. (2011) working on a different set of samples from the Damma chronosequence noted an increase in the proportion of Fe(III) to total Fe from 30% in the unweathered rocks and youngest soils to about 53% in a 140-yr-old soil and showed that this is related to the formation of Fe(III)-bearing phyllosilicates and Fe(III) (hydr)oxides. These subtle changes, however, cannot be detected by X-ray diffraction analysis, but demonstrate ongoing formation of pedogenic minerals. These findings are in agreement with results from Egli et al. (2003) and Mavris et al. (2010). These authors found that in soils developed on granitic parent material, conversion of biotite to hydrobiotite and other changes in soil clay mineralogy can be detected after about 150 yr. The formation of smectite and hydroxy-interlayered smectite was especially pronounced in soils older than 100 yr (i.e., at Sites 17–24). These mineralogical changes are not clearly reflected in changes in the bulk chemical composition of the soils due to the small proportion of the clay fraction.

The decrease of soil pH along the chronosequence clearly indicates ongoing soil acidification in the glacier forefield. This supports earlier studies in other deglaciation chronosequences (Burt and Alexander, 1996; Darmody et al., 2005; He and Tang, 2008) that postulated leaching of organic acids resulting from SOM degradation as the main source of soil acidification. The pH decrease was also evident in volcanic chronosequences (Lilienfein et al., 2003; Kato et al., 2005), while BS was constant (Kato et al., 2005). Ongoing soil acidification is also reflected in the decrease in BS with increasing soil acidification as a result of preferential leaching of base cations (Na^+, K^+, Ca^{2+}, and Mg^{2+}). In the 0- to 5-cm layer, this trend is counteracted by nutrient cycling within the plant–rhizosphere system resulting in higher BS values compared to the respective 5- to 10-cm layers. Soil acidification is known to affect the CEC. Due to increasing protonation of surface sites with pH-variable charge, the effective CEC is expected to decrease with decreasing soil pH. However, a clearly opposite trend was observed in this study. An increasing CEC despite ongoing acidification could be explained by formation of secondary minerals having a considerably higher CEC than the unweathered parent material and by the accumulation of organic matter. Formation of secondary minerals exhibiting a high CEC was not observed to occur to a substantial extent along the chronosequence (see above), whereas accumulation of organic matter is clearly visible (Fig. 5). While in the Damma glacier forefield all soils contain exchangeable Al (data not shown), at the Mendenhall Glacier in Alaska—also on acid bedrock—only soils older than 70 yr exhibited detectable amounts of exchangeable Al (Burt and Alexander, 1996). The good correlation between CEC and organic C content within the chronosequence ($CEC = 6.4 + 1106 \times C_{org}$; $R^2 = 0.78$) suggests that CEC is mostly linked with SOM. This is supported by a comparison between measured CEC and CEC of SOM estimated as:

$$CEC_{org}\,[mmol_c\,kg^{-1}] = C_{org}\,[kg\,kg^{-1}] \times 1.72 \times 1500 \qquad [2]$$

assuming an average C content of 58% for the SOM in the forefield and a low average exchange capacity of 1500 $mmol_c\,kg^{-1}$ SOM.

The estimation of CEC_{org} by Eq. [2] shows that in the 0- to 5-cm layer, SOM may contribute to soil CEC by about 50% at Sites 1, 2, and 5 (data not shown). In older sites, CEC in the 0- to 5-cm layer is almost exclusively explained by the presence of organic matter. In the 5- to 10-cm layer, the contribution of SOM in most cases is lower than in the surface layer. However, its contribution to subsoil CEC also increases with soil age and at the sites that are older than 60 yr, CEC is thus explained to a large extent, if not almost exclusively, by SOM. The large attribution of CEC_{eff} to SOM supports earlier findings at other chronosequences defined by deglaciation (Burt and Alexander, 1996; Darmody et al., 2005; He and Tang, 2008) or volcanic eruptions (Kato et al., 2005; Lilienfein et al., 2003). The values of CEC_{eff} of up to 60 $mmol_c\ kg^{-1}$ found in our study are small compared to those found in the other deglaciation chronosequences, two of which are on acid bedrock and one on carbonate containing bedrock (He and Tang, 2008). Our CEC_{eff} values are more comparable to those found on volcanic material.

The similarity of the older Sites 15 and 20 to the youngest sites with respect to pH and CEC_{eff} could be related to disturbance from sediment transport, to the somewhat higher clay contents, or to the relatively wet conditions of these sites, although this is not clearly apparent in other parameters.

An exponential increase of SOM concentrations has been observed before in other locations with initial soil buildup (Conen et al., 2007; Zehetner et al., 2009). Essentially, an exponential growth of the whole ecosystem takes place, without any leveling off due to adverse effects like a possible increase in degradation of SOM or competition among plants. The resetting of the TOC contents in the intermediate-age samples (Fig. 7) is due to a combination of two factors. For Sites 5 and 6 there are clear indications that the TOC content has been reduced by addition of fresh sediment during the glacier re-advance and melting, thus diluting the organic C to values similar to the newly exposed samples. For other sites a dilution effect cannot be clearly identified, and the decrease in TOC can also be due to the relatively high proportion of labile organic matter in these soils (Smittenberg et al., unpublished data, 2011). These authors show that most of the organic matter in the forefield is easily oxidizable, with a short turnover time (year to decadal); thus, TOC of the soils would be reduced when organic C input was lower during glacier re-advances. In addition, this shows that recalcitrant organic matter is not formed in significant amounts in this environment at decadal time scales.

Biotic Characteristics

All biological variables indicate that in spite of the strong heterogeneity of the system our sampling strategy successfully captured the temporal development of the ecosystem. It evolves from sandy soils with a few individual pioneer plants to an ecosystem with almost complete vegetation cover in less than 70 yr, and to soils with a clear structure within approximately 100 yr. Whereas plant species richness increases with soil age, the Shannon diversity of the vegetation is already rather high at the youngest sites; i.e., there are not many plants in the pioneer stages, but the ones present often belong to different species. As in other glacier forefields (cf. Ellenberg, 1986; Chapin et al., 1994; Erschbamer et al., 1999), after 100 yr the vegetation is already dominated by woody plants such as *Salix* spp. or *Rhododendron ferrugineum* which have associations with (mostly) ecto- and ericoid mycorrhizal fungi, respectively. However, individual seedlings of *Salix* spp. occur already at the youngest sites (7–8 yr) and form ectomycorrhizal associations there (data not shown). In contrast, herbaceous plants on the youngest sites had no arbuscular mycorrhiza yet or the colonization density was very low (e.g., 5 and 12% for *Poa alpina* L. at 7 and 8 yr after deglaciation, respectively) (Welc et al., unpublished data, 2010). The biomass and vegetation cover, as well as soil development, could probably have been even faster if the two glacier re-advances had not influenced the development, at least in the vicinity of the end moraines, as seen in the C content of the soil.

Both density and species richness of testate amoebae increased over the chronosequence. This pattern agrees with a comparable study in a proglacial chronosequence in Alaska (Carlson et al., 2010) and is in accordance with the hypothesis that the diversity of soil organisms increases with increasing ecosystem net photosynthetic production (Wardle, 2002). The buildup of C in the soil is probably an important factor governing the development of testate amoeba communities, since these protists contribute significantly to the mineralization of C (and other nutrients) in soils (Schröter et al., 2003). However, testate amoebae are aquatic organisms living in the water film in the soil environment, and their density and community structure are usually primarily determined by moisture level or water table depth in both peatlands and mineral soils (Lousier, 1974; Mitchell et al., 2008). Therefore, the observed changes may also relate to changes in soil physical characteristics (i.e., increasing content of clay and silt in older sites) and changes in microclimatic conditions.

Microbial biomass was determined by two different methods, namely PLFA and microbial C, P, and N determination in fumigated soils. There is only a relatively weak correlation between the two methods to quantify microbial biomass because, among other factors, they do not treat the dormant and active components equivalently (Ohtonen et al., 1999). Thus, these data should be used with caution when inferring changes in microbial abundances. However, both PLFAs and microbial C extracted by fumigation clearly show a pattern of increase with age (Fig. 11), which closely follows TOC contents (Fig. 7), and therefore appear to be generally driven by the soil organic matter buildup with time. The Shannon diversity indices from T-RFLP profiling indicated that bacterial communities were diverse in the Damma glacier forefield, but that diversity remains rather constant along the chronosequence. This is in accordance with Schutte et al. (2009), but contradictory to Nemergut et al. (2007), who detected an increase in the diversity with soil age. These differing results suggest that the factors

influencing bacterial diversity are not solely related to the soil age, but also to other factors like climatic conditions, bedrock composition, soil texture, pH (Lazzaro et al., 2009; Mannisto et al., 2007), and the composition of plant communities.

Although diversity does not change significantly, cluster analysis indicated a change of the bacterial community structure from bare to densely vegetated soils, and thus a bacterial succession along this forefield. In the initial phase of colonizing barren soils, bacteria are driven by the chemical composition of the rock. Different minerals are likely colonized by diverse bacteria (Gleeson et al., 2006). Further, bacterial communities are affected by development of plant communities. Therefore, the bacterial community structures change with altering soil parameters and plant colonization (Haemmerli et al., 2007). This shift in the bacterial communities from barren rocks to a humic, vegetated soil was clearly indicated by our T-RFLP profiles. Limited C and N sources on bare soil select for a specific bacterial community. Mainly C and N_2 fixers (Crews et al., 2001; Stibal et al., 2008) and weathering-associated bacteria can survive here (Frey et al., 2010). In the older more developed soils, decomposers of plant material and nitrate reducers are thriving, and the bacteria present in bare soils are probably suppressed (Deiglmayr et al., 2006; Schutte et al., 2009).

Fungi display a much lower diversity than bacteria, as revealed by the T-RFLP analysis. This could have an ecological reason, taking into account that fungi often are tightly associated with plants (e.g., mycorrhizal fungi) and thus have a limited potential to colonize the sparsely vegetated forefield, whereas bacteria have the potential to colonize all the niches available. An additional factor could be also different strategies for spatial and/or temporal dispersion of spores. The reduced diversity of the fungal population could also partly have a methodological explanation because the length of the 16S rRNA gene fragment in bacteria is almost double the corresponding 18S rRNA gene fragment in fungi. Thus, a higher number of peaks and a higher number of digestion patterns in bacteria are likely to occur. Edel-Hermann et al. (2008), applying the same two primer pairs for bacteria and fungi to an agricultural soil, obtained 122 T-RFs and 47 T-RFs for bacteria and fungi, respectively. With respect to the fungal distribution over a soil chronosequence, Jumpponen (2003) found that younger soils contain a higher diversity of fungi than older soils. The author also observed that most T-RFs were located only at one site, indicating the high spatial variability of the fungal populations within the forefield. In our study, the diversity of the fungi was more or less evenly distributed along the chronosequence. However, the compositions of the fungal communities varied greatly due to the different soil ages, as shown by our cluster analysis (Fig. 10).

In contrast to our data, which show an approximately constant ratio of fungi to bacteria along the chronosequence, Ohtonen et al. (1999) observed that the biomass ratio of fungi/bacteria in a glacier chronosequence of Lyman Glacier, covering 80 yr, increases with soil succession. They interpreted this to reflect an increase in C use efficiency, expressed as the proportion of C used to build up biomass vs. respiration. An alternative interpretation was given by Bardgett et al. (2005) (citing older work), who showed that the biomass ratio of fungi/bacteria increases during soil succession and suggested that the young sites are characterized by leaky nutrient cycles, whereas the older sites are more conservative with nutrients. It is difficult to compare these results, because we do not have direct measurements of microbial activity on our samples. However, Sigler et al. (2002) observed that in a different set of soils from the Damma chronosequence bacterial activities reached a maximum in 70-yr-old soils and decreased in older soils. Also a previous study in young soils of the Damma chronosequence (Miniaci et al., 2007) showed that pioneer plants had a significant effect on cell numbers and microbial activity in the rhizosphere of the plants, but not on the community composition. The different biological response of ecosystems under similar conditions calls for further studies focusing specifically on the activity of the microorganisms to explain the evolutionary trajectory of an ecosystem and possible aboveground–belowground interactions. In addition, it is also necessary to consider different temporal fluctuations and conduct sampling at different timescales (daily to seasonal) to obtain a better understanding of the relationships between microbial groups and belowground and aboveground ecology (Bardgett et al., 2005). Our results lead to the conclusions that the forefield of the Damma glacier is densely populated with microorganisms and that the amount of bacterial and fungal species does not strongly differ when nonvegetated soils are compared with vegetated soils. For a quantitative estimate of microbial biomass, different methods should be employed to obtain a more solid estimate of microbial biomass.

Conclusions and Outlook

This first summary of our multidisciplinary studies of the Damma glacier forefield soil chronosequence provides a clear documentation of the gradients present in the forefield in many parameters. This shows that, in spite of the strong spatial heterogeneity of this kind of ecosystems we were successful in capturing clear gradients related to the temporal evolution of this ecosystem. While the mineralogy and elemental composition of the soils is rather homogeneous, biological ecosystem evolution is much more rapid. Only in older soils (>100 yr) is incipient weathering observed, shown mainly by a decreasing content in plagioclase and biotite weathering and coincidental formation of secondary chlorites.

As observed in other studies, soils develop from bare parent material to structured soil with litter layer and some zoning within a few decades. With the pH decrease some Fe-leaching is sometimes visible in the color zonation of the older soils, but leaching is very minor and is not reflected in the bulk composition of the soils. Soil organic C contents increase exponentially with age, but most SOM appears to be relatively labile and thus does not represent a stable C sink over long timescales.

The patterns of observed microbial distribution allow one to infer evolutionary trajectories, but as with many other studies, this work only provides a snapshot of the real evolution of the highly dynamic microbial communities. Only with a much more extensive sampling at a temporal resolution that allows one to capture the response of microorganisms to fluctuating external drivers such as seasonality, moisture changes, slope, and exposure (north–south), which were not considered in this study, will allow better understanding and prediction of the evolution of the ecosystem and interactions between aboveground and belowground ecology. Some of these aspects (e.g., the influence of exposure on microbial communities) are being studied in further ongoing studies with soil translocations.

Acknowledgments

We thank two anonymous reviewers for their constructive comments. This project was funded by the Competence Center Environment and Sustainability of the ETH domain through the project BigLink and internal funding resources of ETH Zürich and Swiss Federal Institute for Forest, Snow and Landscape Research (WSL). All results discussed in this paper are available electronically at http://www.cces.ethz.ch/projects/clench/BigLink/data or from the senior author.

References

Anderson, S.P. 2007. Biogeochemistry of glacial landscape systems. Annu. Rev. Earth Planet. Sci. 35:375–399. doi:10.1146/annurev.earth.35.031306.140033

Anderson, S.P., J.I. Drever, C.D. Frost, and P. Holden. 2000. Chemical weathering in the foreland of a retreating glacier. Geochim. Cosmochim. Acta 64:1173–1189. doi:10.1016/S0016-7037(99)00358-0

Bardgett, R.D., W.D. Bowman, R. Kaufmann, and S.K. Schmidt. 2005. A temporal approach to linking aboveground and belowground ecology. Trends Ecol. Evol. 20:634–641. doi:10.1016/j.tree.2005.08.005

Baumler, R., D.P. Madhikermi, and W. Zech. 1997. Fine silt and clay mineralogical changes of a soil chronosequence in the Langtang valley (Central Nepal). Z. Pflanzener. Bodenkd. 160:413–421. doi:10.1002/jpln.19971600311

Becker, T., and H. Dierschke. 2005. Primary succession on the forefield of the Obersulzbachkees Glacier (Hohe Tauern, Austria): A chronosequence of almost 150 years. Tuexenia:111–139.

Bernasconi, S.M., and BigLink project members. 2008. Weathering, soil formation and initial ecosystem evolution on a glacier forefield: A case study from the Damma Glacier, Switzerland. Mineral. Mag. 72:19–22. doi:10.1180/minmag.2008.072.1.19

Bormann, B.T., and R.C. Sidle. 1990. Changes in productivity and distribution of nutrients in a chronosequence at Glacier Bay national park, Alaska. J. Ecol. 78:561–578. doi:10.2307/2260884

Borneman, J., and R.J. Hartin. 2000. PCR primers that amplify fungal rRNA genes from environmental samples. Appl. Environ. Microbiol. 66:4356–4360. doi:10.1128/AEM.66.10.4356-4360.2000

Brindley, G.W., and G. Brown. 1980. Crystal structures of clay minerals and their identification. Mineral. Soc. Monogr. 5. Mineralogical Society, London.

Brunner, I., M. Plotze, S. Rieder, A. Zumsteg, G. Furrer, and B. Frey. 2011. Pioneering fungi from the Damma glacier forefield in the Swiss Alps can promote granite weathering. Geobiology 9:266–279. doi:10.1111/j.1472-4669.2011.00274.x

Burt, R., and E.B. Alexander. 1996. Soil development on moraines of Mendenhall Glacier, southeast Alaska.2. Chemical transformations and soil micromorphology. Geoderma 72:19–36. doi:10.1016/0016-7061(96)00022-5

Carlson M.L., L.A. Flagstad, F. Gillet, and E.A.D. Mitchell. 2010. Community development along a proglacial chronosequence: Are above-ground and below-ground community structure controlled more by biotic than abiotic factors? J. Ecol. 98:1084-1095. doi:10.1111/j.1365-2745.2010.01699.x.

Chapin, F.S., III, L.R. Walker, C.L. Fastie, and L.C. Sharman. 1994. Mechanisms of primary succession following deglaciation at Glacier Bay, Alaska. Ecol. Monogr. 64:149–175. doi:10.2307/2937039

Conen, F., M.V. Yakutin, T. Zumbrunn, and J. Leifeld. 2007. Organic carbon and microbial biomass in two soil development chronosequences following glacial retreat. Eur. J. Soil Sci. 58:758–762. doi:10.1111/j.1365-2389.2006.00864.x

Crews, T.E., L.M. Kurina, and P.M. Vitousek. 2001. Organic matter and nitrogen accumulation and nitrogen fixation during early ecosystem development in Hawaii. Biogeochemistry 52:259–279. doi:10.1023/A:1006441726650

Darmody, R.G., C.E. Allen, and C.E. Thorn. 2005. Soil topochronosequences at Storbreen, Jotunheimen, Norway. Soil Sci. Soc. Am. J. 69:1275–1287. doi:10.2136/sssaj2004.0204

de Souza, G.F., B.C. Reynolds, M. Kiczka, and B. Bourdon. 2010. Evidence for mass-dependent isotopic fractionation of strontium in a glaciated granitic watershed. Geochim. Cosmochim. Acta 74:2596–2614. doi:10.1016/j.gca.2010.02.012

Deiglmayr, K., L. Philippot, D. Tscherko, and E. Kandeler. 2006. Microbial succession of nitrate-reducing bacteria in the rhizosphere of *Poa alpina* across a glacier foreland in the Central Alps. Environ. Microbiol. 8:1600–1612. doi:10.1111/j.1462-2920.2006.01051.x

Doblas-Miranda, E., D.A. Wardle, D.A. Peltzer, and G.W. Yeates. 2008. Changes in the community structure and diversity of soil invertebrates across the Franz Josef Glacier chronosequence. Soil Biol. Biochem. 40:1069–1081. doi:10.1016/j.soilbio.2007.11.026

Dolezal, J., K. Homma, K. Takahashi, M.P. Vyatkina, V. Yakubov, V.P. Vetrova, and T. Hara. 2008. Primary succession following deglaciation at Koryto Glacier Valley, Kamchatka. Arct. Antarct. Alp. Res. 40:309–322. doi:10.1657/1523-0430(06-123)[DOLEZAL]2.0.CO;2

Duc, L., M. Noll, B.E. Meier, H. Burgmann, and J. Zeyer. 2009. High diversity of diazotrophs in the forefield of a receding alpine glacier. Microb. Ecol. 57:179–190. doi:10.1007/s00248-008-9408-5

Edel-Hermann, V., N. Gautheron, C. Alabouvette, and C. Steinberg. 2008. Fingerprinting methods to approach multitrophic interactions among microflora and microfauna communities in soil. Biol. Fertil. Soils 44:975–984. doi:10.1007/s00374-008-0287-1

Egli, M., A. Mirabella, and P. Fitze. 2003. Formation rates of smectites derived from two Holocene chronosequences in the Swiss Alps. Geoderma 117:81–98. doi:10.1016/S0016-7061(03)00136-8

Egli, M., M. Wernli, C. Kneisel, and W. Haeberli. 2006. Melting glaciers and soil development in the proglacial area Morteratsch (Swiss Alps): I. Soil type chronosequence. Arct. Antarct. Alp. Res. 38:499–509. doi:10.1657/1523-0430(2006)38[499:MGASDI]2.0.CO;2

Egli, M., C. Mavris, A. Mirabella, and D. Giaccai. 2010. Soil organic matter formation along a chronosequence in the Morteratsch proglacial area (Upper Engadine, Switzerland). Catena 82:61–69. doi:10.1016/j.catena.2010.05.001

Ellenberg, H. 1986. Vegetation mitteleuropas mit den Alpen. Ulmer, Stuttgart.

Erschbamer, B., W. Bitterlich, and C. Rafel. 1999. The vegetation as an indicator of soil development on the glacier foreland of the Rotmoosferner (Obergurgl, Nothern Tyrol). Ber. Nat. Med. Verein Innsbruck 86:107–122.

Fastie, C.L. 1995. Causes and ecosystem consequences of multiple pathways of primary succession at Glacier Bay, Alaska. Ecology 76:1899–1916. doi:10.2307/1940722

Frey, B., M. Stemmer, F. Widmer, J. Luster, and C. Sperisen. 2006. Microbial activity and community structure of a soil after heavy metal contamination in a model forest ecosystem. Soil Biol. Biochem. 38:1745–1756. doi:10.1016/j.soilbio.2005.11.032

Frey, B., S.R. Rieder, I. Brunner, M. Plotze, S. Koetzsch, A. Lapanje, H. Brandl, and G. Furrer. 2010. Weathering-associated bacteria from the Damma Glacier forefield: Physiological capabilities and impact on granite dissolution. Appl. Environ. Microbiol. 76:4788–4796. doi:10.1128/AEM.00657-10

Frostegard, A., and E. Baath. 1996. The use of phospholipid fatty acid analysis to estimate bacterial and fungal biomass in soil. Biol. Fertil. Soils 22:59–65. doi:10.1007/BF00384433

Frostegard, A., A. Tunlid, and E. Baath. 1991. Microbial biomass measured as total lipid phosphate in soils of different organic content. J. Microbiol. Methods 14:151–163. doi:10.1016/0167-7012(91)90018-L

Gee, G.W., and J.W. Bauder. 1979. Particle-size analysis by hydrometer—Simplified method for routine textural analysis and a sensitivity test of measurement parameters. Soil Sci. Soc. Am. J. 43:1004–1007. doi:10.2136/sssaj1979.03615995004300050038x

Gleeson, D.B., N.M. Kennedy, N. Clipson, K. Melville, G.M. Gadd, and F.P. McDermott. 2006. Characterization of bacterial community structure on a weathered pegmatitic granite. Microb. Ecol. 51:526–534. doi:10.1007/s00248-006-9052-x

Haemmerli, A., S. Waldhuber, C. Miniaci, J. Zeyer, and M. Bunge. 2007. Local expansion and selection of soil bacteria in a glacier forefield. Eur. J. Soil Sci. 58:1437–1445. doi:10.1111/j.1365–2389.2007.00948.x

He, L., and Y. Tang. 2008. Soil development along primary succession sequences on moraines of Hailuogou Glacier, Gongga Mountain, Sichuan, China. Catena 72:259–269. doi:10.1016/j.catena.2007.05.010

Heuer, H., M. Krsek, P. Baker, K. Smalla, and E.M.H. Wellington. 1997. Analysis of actinomycete communities by specific amplification of genes encoding 16S rRNA and gel-electrophoretic separation in denaturing gradients. Appl. Environ. Microbiol. 63:3233–3241.

Hill, M.O. 1973. Diversity and evenness—Unifying notation and its consequences. Ecology 54:427–432. doi:10.2307/1934352

Hindshaw, R.S., B.C. Reynolds, J.G. Wiederhold, R. Kretzschmar, and B. Bourdon. 2011a. Calcium isotopes in a proglacial weathering environment: Damma glacier, Switzerland. Geochim. Cosmochim. Acta 75:106–118. doi:10.1016/j.gca.2010.09.038

Hindshaw, R.S., E.T. Tipper, B.C. Reynolds, E. Lemarchand, J.G. Wiederhold, J. Magnusson, S. Bernasconi, R. Kretzschmar, and B. Bourdon. 2011b. Hydrological control of stream water chemistry in a glacial catchment (Damma Glacier, Switzerland). Chem. Geol. 285:215–230. doi:10.1016/j.chemgeo.2011.04.012

IUSS Working Group WRB. 2006. World reference book for soil resources. World Soil Resour. Rep. 103. FAO, Rome

Jumpponen, A. 2003. Soil fungal community assembly in a primary successional glacier forefront ecosystem as inferred from rDNA sequence analyses. New Phytol. 158:569–578. doi:10.1046/j.1469-8137.2003.00767.x

Kates, M. 1986. Lipid extraction procedures. p. 100–111. *In* Techniques of lipidology: Isolation, analysis and identification of lipids. 2nd ed. Elsevier Science Publishers B.V, Amsterdam.

Kato, T., T. Kamijo, T. Hatta, K. Tamura, and T. Higashi. 2005. Initial soil formation processes of volcanogenous regosols (Scoriacious) from Miyake-Jima Island, Japan. Soil Sci. Plant Nutr. 51:291–301. doi:10.1111/j.1747-0765.2005.tb00033.x

Kiczka, M., J.G. Wiederhold, S.M. Kraemer, B. Bourdon, and R. Kretzschmar. 2010. Iron isotope fractionation during Fe uptake and translocation in alpine plants. Environ. Sci. Technol. 44:6144–6150. doi:10.1021/es100863b

Kiczka, M., J.G. Wiederhold, J. Frommer, A. Voegelin, S.M. Kraemer, B. Bourdon, and R. Kretzschmar. 2011. Iron speciation and isotope fractionation during silicate weathering and soil formation in an alpine glacier forefield chronosequence. Geochim. Cosmochim. Acta (in press). doi:0.1016/j.gca.2011.07.008

Kiczka, M. 2011. Iron isotope fractionation mechanisms of silicate weathering and iron cycling by plants. PhD. diss. ETH Zürich. doi:10.3929/ethz-a-006353249.

Kouno, K., Y. Tuchiya, and T. Ando. 1995. Measurement of soil microbial biomass phosphorus by an anion-exchange membrane method. Soil Biol. Biochem. 27:1353–1357. doi:10.1016/0038-0717(95)00057-L

Lazzaro, A., C. Abegg, and J. Zeyer. 2009. Bacterial community structure of glacier forefields on siliceous and calcareous bedrock. Eur. J. Soil Sci. 60:860–870 doi:10.1111/j.1365-2389.2009.01182.x

Lilienfein, J., R.G. Qualls, S.M. Uselman, and S.D. Bridgham. 2003. Soil formation and organic matter accretion in a young andesitic chronosequence at Mt. Shasta, California. Geoderma 116:249–264. doi:10.1016/S0016-7061(03)00086-7

Lousier, J.D. 1974. Response of soil testacea to soil-moisture fluctuations. Soil Biol. Biochem. 6:235–239. doi:10.1016/0038-0717(74)90057-1

Magnusson, J., D. Farinotti, T. Jonas, and M. Bavay. 2011. Quantitative evaluation of different hydrological modeling approaches in a partly glacierized Swiss watershed. Hydrol. Processes 25:2071–2084. doi:10.1002/hyp.7958

Magnusson, J., T. Jonas, I. Lopez-Moreno, and M. Lehning. 2010. Snow cover response to climate change in a high alpine and half-glacierized basin in Switzerland. Hydrol. Res. 41:230–240. doi:10.2166/nh.2010.115

Mannisto, M.K., M. Tiirola, and M.M. Haggblom. 2007. Bacterial communities in Arctic fjelds of Finnish Lapland are stable but highly pH-dependent. FEMS Microbiol. Ecol. 59:452–465 doi:10.1111/j.1574-6941.2006.00232.x

Mavris, C., M. Egli, M. Plotze, J.D. Blum, A. Mirabella, D. Giaccai, and W. Haeberli. 2010. Initial stages of weathering and soil formation in the Morteratsch proglacial area (Upper Engadine, Switzerland). Geoderma 155:359–371. doi:10.1016/j.geoderma.2009.12.019

Miniaci, C., M. Bunge, L. Duc, I. Edwards, H. Burgmann, and J. Zeyer. 2007. Effects of pioneering plants on microbial structures and functions in a glacier forefield. Biol. Fertil. Soils 44:289–297. doi:10.1007/s00374-007-0203-0

Mitchell, E.A.D., D.J. Charman, and B.G. Warner. 2008. Testate amoebae analysis in ecological and paleoecological studies of wetlands: Past, present and future. Biodivers. Conserv. 17:2115–2137. doi:10.1007/s10531-007-9221-3

National Research Council Committee on Basic Research Opportunities in the Earth Sciences. 2001. Basic research opportunities in the earth sciences. National Academies Press, Washington, DC.

Nemergut, D.R., S.P. Anderson, C.C. Cleveland, A.P. Martin, A.E. Miller, A. Seimon, and S.K. Schmidt. 2007. Microbial community succession in an unvegetated, recently deglaciated soil. Microb. Ecol. 53:110–122. doi:10.1007/s00248-006-9144-7

Ohtonen, R., H. Fritze, T. Pennanen, A. Jumpponen, and J. Trappe. 1999. Ecosystem properties and microbial community changes in primary succession on a glacier forefront. Oecologia 119:239–246. doi:10.1007/s004420050782

Poerschmann, J., and R. Carlson. 2006. New fractionation scheme for lipid classes based on "in-cell fractionation" using sequential pressurized liquid extraction. J. Chromatogr. A 1127:18–25. doi:10.1016/j.chroma.2006.07.063

Rietveld, H.M. 1969. A profile refinement method for nuclear and magnetic structures. J. Appl. Cryst. 2:65–71. doi:10.1107/S0021889869006558

Schaltegger, U. 1990. The central Aar granite—Highly differentiated calc-alkaline magmatism in the Aar massif (Central Alps, Switzerland). Eur. J. Mineral. 2:245–259.

Schmalenberger, A., and M. Noll. 2010. Shifts in desulfonating bacterial communities along a soil chronosequence in the forefield of a receding glacier. FEMS Microbiol. Ecol. 71:208–217. doi:10.1111/j.1574-6941.2009.00799.x

Schmidt, S.K., S.C. Reed, D.R. Nemergut, A.S. Grandy, C.C. Cleveland, M.N. Weintraub, A.W. Hill, E.K. Costello, A.F. Meyer, J.C. Neff, and A.M. Martin. 2008. The earliest stages of ecosystem succession in high-elevation (5000 metres above sea level), recently deglaciated soils. Proc. R. Soc. B Biol. Sci. 275:2793–2802. doi:10.1098/rspb.2008.0808.

Schröter, D., V. Wolters, and P.C. De Ruiter. 2003. C and N mineralisation in the decomposer food webs of a European forest transect. Oikos 102:294–308.

Schutte, U.M.E., Z. Abdo, S.J. Bent, C.J. Williams, G.M. Schneider, B. Solheim, and L.J. Forney. 2009. Bacterial succession in a glacier foreland of the High Arctic. ISME J. 3:1258–1268. doi:10.1038/ismej.2009.71

Sigler, W.V., S. Crivii, and J. Zeyer. 2002. Bacterial succession in glacial forefield soils characterized by community structure, activity and opportunistic growth dynamics. Microb. Ecol. 44:306–316. doi:10.1007/s00248-002-2025-9

Sigler, W.V., and J. Zeyer. 2002. Microbial diversity and activity along the forefields of two receding glaciers. Microb. Ecol. 43:397–407. doi:10.1007/s00248-001-0045-5

Soil Survey Staff. 2010. Keys to soil taxonomy. 11th ed. NRCS, Washington, DC.

Stibal, M., M. Tranter, L.G. Benning, and J. Rehak. 2008. Microbial primary production on an Arctic glacier is insignificant in comparison with allochthonous organic carbon input. Environ. Microbiol. 10:2172–2178. doi:10.1111/j.1462-2920.2008.01620.x

Stockmarr, J. 1971. Tablets with spores in absolute pollen analysis. Pollen Spores 13:615–621.

Vance, E.D., P.C. Brookes, and D.S. Jenkinson. 1987. An extraction method for measuring soil microbial biomass-C. Soil Biol. Biochem. 19:703–707. doi:10.1016/0038-0717(87)90052-6

Walker, R.L., and R. del Moral. 2003. Primary succession and ecosystem rehabilitation. Cambridge Univ. Press, Cambridge, UK.

Walker, L.R., D.A. Wardle, R.D. Bardgett, and B.D. Clarkson. 2010. The use of chronosequences in studies of ecological succession and soil development. J. Ecol. 98:725–736. doi:10.1111/j.1365-2745.2010.01664.x

Wardle, D.A. 2002. Communities and ecosystems: Linking the aboveground and belowground components. Princeton Univ. Press, Princeton, NJ.

Wilkinson, D.M. 2008. Testate amoebae and nutrient cycling: Peering into the black box of soil ecology. Trends Ecol. Evol. 23:596–599. doi:10.1016/j.tree.2008.07.006

Zehetner, F., G.J. Lair, and M.H. Gerzabek. 2009. Rapid carbon accretion and organic matter pool stabilization in riverine floodplain soils. Global Biogeochem. Cycl. 23. GB4004, doi:10.1029/2009GB003481